To What Extent Do Extreme Storm Events Change Future Flood Hazards?

Mariam Khanam[1], Giulia Sofia[1], and Emmanouil N. Anagnostou[1]

[1]Civil & Environmental Engineering, University of Connecticut, Storrs, 06269, USA

5

Correspondence to: Mariam Khanam (mariam.khanam@uconn.edu), Giulia Sofia (giulia.sofia@uconn.edu)

- **Abstract.** Due to global climate change, flooding is predicted to become more frequent in the coming decades. Recent
  literature has highlighted the importance of river morphodynamics in controlling flood hazards at the local scale.
  Abrupt and short-term geomorphic changes can occur after major storms. However, our ability to foresee where and
10 when substantial changes will happen is still limited, hindering our understanding of their ramifications on future
  flood hazards. This study sought to understand the implications of major storm events for future flood hazards. For
  this purpose, we developed self-organizing maps (SOMs) to predict post-storm changes in stage-discharge
  relationships, based on storm characteristics and watershed properties at 3,101 stream gages across the continental
  United States (CONUS). We tested and verified a machine learning (ML) model and its feasibility for (1) mapping
15 the variability of geomorphic impacts of extreme storm events and (2) representing the effects of these changes on
  stage-discharge relationships at gaged sites as a proxy for changes in flood hazard. The established model allows us
  to select rivers with stage-discharge relationships that are more prone to change after severe storms, for which flood
  frequency analysis should be revised on a regular basis so that hazard assessment can be up to date with the changing
  conditions. Results from the model show that, even though post-storm changes in channel conveyance are widespread,
20 the impacts on flood hazard vary across CONUS. The influence of channel conveyance variability on flood risk
  depends on various parameters characterizing a particular landscape or storm. The proposed framework can serve as
  a basis for incorporating channel conveyance adjustments into flood hazard assessment.

1 Introduction

Several factors contribute to the non-stationarity in flow regimes, including variations in human activities, changes
25 in land cover and land use, climate changes, and low-frequency internal climate variability (i.e., multidecadal oscillations)
(Cunderlik and Burn, 2003; Mostofi Zadeh et al., 2020). Consequently, flood trends over the past decades have changed
worldwide (Chang et al., 2007; FEMA, 2013; Karagiannis et al., 2017; McEvoy et al., 2012; Ziervogel et al., 2014), with
critical impacts on society and the environment (Blöschl et al., 2019; Dottori et al., 2022, 2018; Hattermann et al., 2014; Milly
et al., 2002; Mostofi Zadeh et al., 2020; Slater et al., 2015).

30   Traditional "cause-effect" studies have focused on the time dependency or non-stationarity of individual hydrologic flood drivers (Alfieri et al., 2015; Khanam et al., 2021; Lisenby and Fryirs, 2016; Mallakpour and Villarini, 2015; Mostofi Zadeh et al., 2020; Munoz et al., 2018). However, these studies might be under or overestimating the actual damage, especially in regions where the landscape is changing rapidly.

For decades, fluvial geomorphology research has focused on changes in river characteristics (Baker, 1994; Benito and Hudson, 2010; Stott, 2013). River channels and their adjacent floodplains continuously evolve because of the interactions of hydrology, landscape, and climate drivers and the interdependencies of processes at different spatial and temporal scales (Lane et al., 2007; Pinter et al., 2006b; Slater et al., 2015; Stover and Montgomery, 2001; Blench 1906-1993, 1969). Humans also critically modify the landscape, contributing to these intricate geomorphic dynamics of rivers and floods (Ceola et al., 2019; Grill et al., 2019; Wohl, 2019).

40   Nonetheless, flood risk measurement has traditionally been based on flood frequency, derived from variability in streamflow, assuming constant channel capacity (Merz et al., 2012; Slater et al., 2015). Various recent works (Ahrendt et al., 2022; Naylor et al., 2016; Slater et al., 2015, 2019; Sofia and Nikolopoulos, 2020a; Sofia et al., 2020) have suggested the time has come to move beyond flood hazard assessment based on this "fixed river" idea.

Even though the amount of water that flows through the river systems during floods does not change, changes in rivers' capability to hold and transport flood waters downstream (river conveyance capacity) impact the likelihood that floods will topple riverbanks or flood defenses. Therefore, these changes in channel capacity alter flood properties, even when flood frequency remains unchanged (Blench 1906-1993, 1969; Criss and Shock, 2001; Lane et al., 2007; Neuhold et al., 2009; Pinter et al., 2008; Slater et al., 2015c; Stover and Montgomery, 2001). Some obvious evidence of the effects of channel changes on flood properties has been presented by recurring flooding in different dynamic rivers (Brierley and Fryirs, 2016; Pinter et al., 2001; Zischg et al., 2018; Tate, 2019; Munoz et al., 2018). During these flood events, impacts are most evident at sites where the rivers' channel capacity has been drastically reduced (Munoz et al., 2018; Tate, 2019; Sofia et al., 2020).

Rivers naturally adapt their geometry (i.e., their breadth, depth, and slope) to changes in discharge and sediment in the upstream catchment and the alterations brought on by human activities (Lisenby et al., 2018). Any changes in these characteristics might also alter the frequency and risk of future flooding.

55   Neglecting the possibility of rapid changes in streamflow regime and channel conveyance capacity can conceal short-term shifts in flood threats. For example, Li et al., (2020) demonstrated that long-term trends are actually composed of numerous short-term shifts of much larger magnitude. These transient stages are mostly caused by abrupt deposition or scouring during extreme storm events and are comparable in magnitude to long-term trends in peak streamflow. Additionally, short- and long-term climate variability can, at the same time, impact the streamflow patterns and channel conveyance changes, with the channel form adjusting to precipitation and sediment supply (Death et al., 2015; Rathburn et al., 2017; Ruiz-Villanueva et al., 2018; Scorpio et al., 2018; Surian et al., 2016; Wicherski et al., 2017).

Figure 1, for example, shows changes in Boulder Creek in Colorado before and after a flash flood in 2013. Comparing the channel planform and width, it is evident the channel got wider after the flood. Images from 2015 and 2019 show that the

secondary channel on the right eventually disappeared, and the main channel acquired a more prominent bend than in the 2013

65   image. Such relatively quick alterations have the potential to further modify the geomorphic characteristics of rivers and to

produce feedback that will affect the properties of future floods (depth, frequency, duration, and spatial extent).

Figure 1: Change in channel width in Boulder Creek, Colorado, before (2012) and after (2013-2015-2019) a flash flood in 2013 (© Google Earth imagery). The Discharge reported here is Daily discharge measured at the gage USGS 06730200.

70   Systematic shifts in a river's stage-discharge relationships identify the need for sharp upward revisions in hazard

levels and stage-based flood-frequency analysis. Adjustments to the river stage-discharge relationship account for, at least

partly, climate variability and long-term change. Nonetheless, while some river changes might persist in time, others could be

more sudden and persist for a shorter time frame, like in the case of extreme storms. These short-term changes are difficult to

predict, but they could substantially increase the post-storm hazard, especially in the case of subsequent storms.

75   Understanding the scale and severity of channel changes after major storm events is vital to improving flood

management and building the resilience of critical infrastructure. A comprehensive study that shows the impacts of storm-

induced channel changes on future flood hazards is missing from our current knowledge. Buraas et al., (2014) highlighted our

limited capability to predict where significant geomorphic changes will occur following extreme events. Other authors have

pointed to multidirectional approaches as promising contributions to the analysis of channel response to severe floods and the

80   identification of controlling factors (Rinaldi et al., 2016; Scorpio et al., 2018; Surian et al., 2016; Wicherski et al., 2017; among

others). Nevertheless, these studies are local examples of how storms can alter rivers and consequently flood hazard.

At regional scales, it is often either impracticable or impossible to identify the precise events responsible for periods

of channel shift: at such a level, linking geomorphic cause and effect becomes increasingly difficult. However, this does not

85 negate the requirement to comprehend and recognize short-term geomorphologic and hydrologic behaviours that can exacerbate or mitigate flood threats. For this purpose, the availability of a large dataset representing a wide range of extreme storm characteristics and channel morphology under different boundary conditions, such as underlying climatic, hydrologic, and geomorphologic settings, is crucial.

In this study, we have utilized stage-discharge "Residuals" [temporal changes in the discharge needed to reach a certain flood warning threshold] (Slater et al. 2015) as a proxy of flood hazard change. We sought to understand and predict
90 the effects of extreme storms on these residuals and, consequently, flood hazards. To achieve this, we introduced a modeling framework based on machine learning (ML) (section 2.3) that characterizes the interdependence of flood drivers, including atmospheric drivers (precipitation and storm characteristics), hydrologic drivers (flow, stage), and geomorphologic drivers (channel width, depth, drainage area, geophysical characteristics). Despite some limitations (Karpatne et al., 2019), ML applications are rapidly gaining popularity in the field of hydrology, geomorphology, and climate studies (Bergen et al., 2019;
95 Schlef et al., 2019; Valentine and Kalnins, 2016). Despite some limitations (Karpatne et al., 2019), ML can be beneficial when we develop non-parametric models that represent unknown multi-variate, non-linear relationships by training on historical measurements provided that these models are adequately validated based on measured data, which informs us as to whether ML results are accurate, transferable, and scalable (Houser et al., 2022; Sarker, 2021; Schlef et al., 2019; Sofia, 2020).

This study uses ML to quantify and model the effects of extreme storms on channel conveyance and the impacts on
100 flood hazards. It aims *to*: (1*) map the spatial variability of geomorphic response to extreme storm events*, and (2) *understand the impact of these storms on the stage-discharge relationships at gaged sites as a proxy for changes in flood hazard.* The study provided an independent test of discharge-based results and produced a tool for generating timely short-term updates of flood hazard estimates for dynamic rivers.

2 Materials and Methods

105 ### 2.1 Quantifying the Impact on Flood Hazard

For this study, we used data from 3,101 U.S. Geological Survey (USGS) gaging stations distributed across the continental United States (Figure 2). The dataset allows us to cover a wide range of physiographic and climatic (See Fig. 2) regions.

We selected stations for which were available both historical field-measured data on channel properties and flood
110 stages assigned by the National Weather Service (NWS). The data for channel properties were retrieved following a procedure developed by (Slater, 2016; Slater et al., 2015) and using the codes provided by the authors at https://github.com/LouiseJSlater/Hydromorphology.
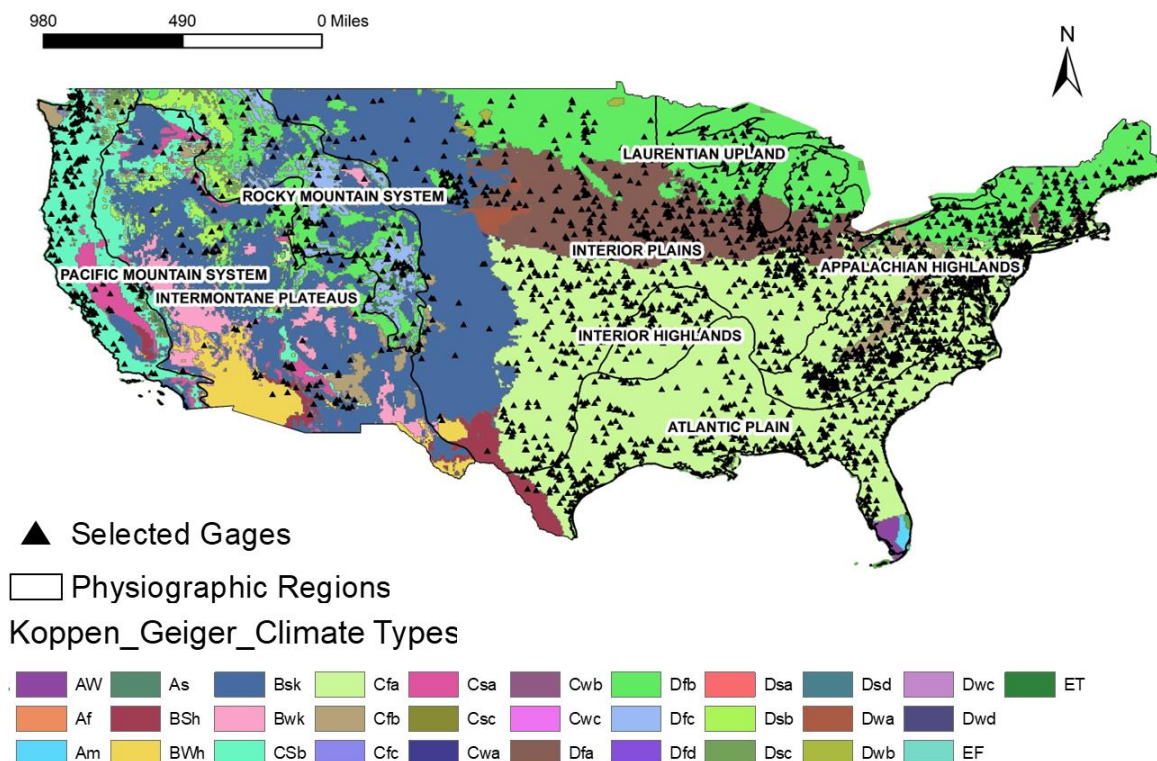
Figure 2: USGS gage stations considered in this study overlain on physiographic and climatic regions-Appalachian Highlands (ApHigh), Atlantic Plain (AtlPlain), Interiors Highlands (IntHigh), Interior Plains (IntPlain), Intermontane Plateaus (IntermPlat), Laurentian Upland (LaurUpl), Pacific Mountain System (PacMounSys), and Rocky Mountain System (RockMounSys); and on Climatic types- Tropical Rainforest (AF), Tropical Monsoon (Am), Tropical Savanna (Wet and Dry Climate) (Aw), Hot Desert Climate (BWh), Cold Desert Climate (BWk), Hot Semi-Arid Climate (BSh), Cold Semi-Arid Climate (BSk), Hot-Summer Mediterranean Climate (Csa), Warm-Summer Mediterranean Climate (Csb), Temperate, dry summer, cold summer (Csc), Warm Oceanic Climate / Humid Subtropical Climate (Cwa), Subtropical highland climate or temperate oceanic climate with dry winters (Cwb), Cold subtropical highland/Subpolar Oceanic (Cwc), Humid Subtropical Climate(Cfa), Temperate Oceanic Climate (Cfb), Subpolar Oceanic ClimateDsa - Humid Continental Climate - Dry Warm Summer (Cfc), Humid Continental Climate - Dry Cool Summer (Dsb), Continental Subarctic - Cold Dry Summer (Dsc), Continental Subarctic – Dry Summer, Very Cold Winter (Dsd), Humid Continental Hot Summers With Dry Winters, Humid Continental Mild Summer With Dry Winters (Dwb), Subarctic With Cool Summers (Dwc). Dry Winters (Dwa), Humid Continental Hot Summers With Year Around Precipitation (Dfa), Humid Continental Mild Summer, Wet All Year (Dfb), Subarctic With Cool Summers And Year Around Rainfall (Dfc), Subarctic With Cold Winters And Year Around Rainfall (Dfd), Tundra Climate (ET), Ice Cap Climate) (EF).

To model the average state of conveyance capacity for each stream gage site, we used theoretical single-stage-discharge relationships (rating curves) at the height associated with the Flood stage, as described by Slater et al. (2015). The flood stage, for the US National Weather Service, indicates a gauge height above which water level begins to impact lives and human activities, and it generally corresponds to the first flood warning threshold. The procedure, therefore, can be adapted for other gage datasets, in different parts of the world, by assuming similar warning thresholds.

5

Deviations from the theoretical stage-discharge relationship indicate that a different stage-discharge relationship
135 existed at a moment in time, which highlights that there might have been temporal changes in channel conveyance. As
described by Li et al. (2020), Slater et al. (2015, 2019), and Slater and Villarini, (2016), using a constant flood level enables
the quantification of "conveyance residuals (Res)" whose variability represents temporal changes in the discharge needed to
reach such a warning threshold (i.e., due to shifts in channel capacity). In a temporal analysis of residuals, a positive to negative
shift indicates a sudden decrease in channel capacity and a potential increase in flood hazard (Slater et al., 2015), as a lower
140 discharge is needed to meet the warning threshold. We followed this procedure to capture the sudden changes in channel
conveyance following major storm events.

To define the stage-discharge relationship, we used a Locally Weighted Scatterplot Smoothing (LOESS) fitting
(Cleveland, 1979), as suggested by Li et al. (2020), Slater et al. (2015, 2019), and Slater and Villarini (2016). The fitting
requires the definition of a smooth parameter, which we set automatically based on the bias-corrected Akaike Information
145 Criterion (AIC) (Hurvich et al., 1998). We performed the analysis using the R package fANCOVA (https://CRAN.R-
project.org/package=fANCOVA).

Before performing the above-mentioned steps, we excluded from the analysis measurements taken prior to the most
recent datum change, if any reported measurement datum change was provided. We did not consider stations with gaps in the
measurements. For the fitting, we only kept field data having discharge within a range of half the flood stage depth on either
150 side of the flood stage, as suggested in Slater et al. (2015). We evaluated the readings visually to look for clusters of outliers
in the scatterplots of the channel measurements that could be signs of changes in the measurement location (or datum). We
eliminated these measurement in a systematic manner. Figure 3 provides an example of changes in residuals after a major
storm event for the Quinnipiac River in Connecticut. From April 15 to April 18, 2007, a spring storm hit the East Coast of the
United States. The streamflow-gaging station recorded flood levels during this occurrence that were more than 0.2 meters
155 higher than the FEMA-projected 100-year levels (Ahearn, 2009). In figure. 3a, the stage and discharge data retrieved from
field measurements taken after the flood appear to shift toward higher values of the stage for comparable discharges compared
to before 2007. The curve fitted at the flood stage (black line in Figure. 3a) ultimately aligns between the two sets of data.
Looking at the residuals concerning the fitted curve (Figure. 3b), the shift from positive residuals, before 2007, to negative is
noticeable. This suggests a loss of conveyance capacity due to deposition, assuming no changes in velocity. The time series of
160 widths (Figure. 3c) and cross-sectional area (Figure. 3d) confirm this loss of conveyance; for this site, slightly changed channel
widths (Figure. 3c) and an abrupt change in capacity (Figure. 3d) can be seen, possibly due to deposition along the riverbed.
Such a change may result in a potential increase in flood hazard for a given flood volume.
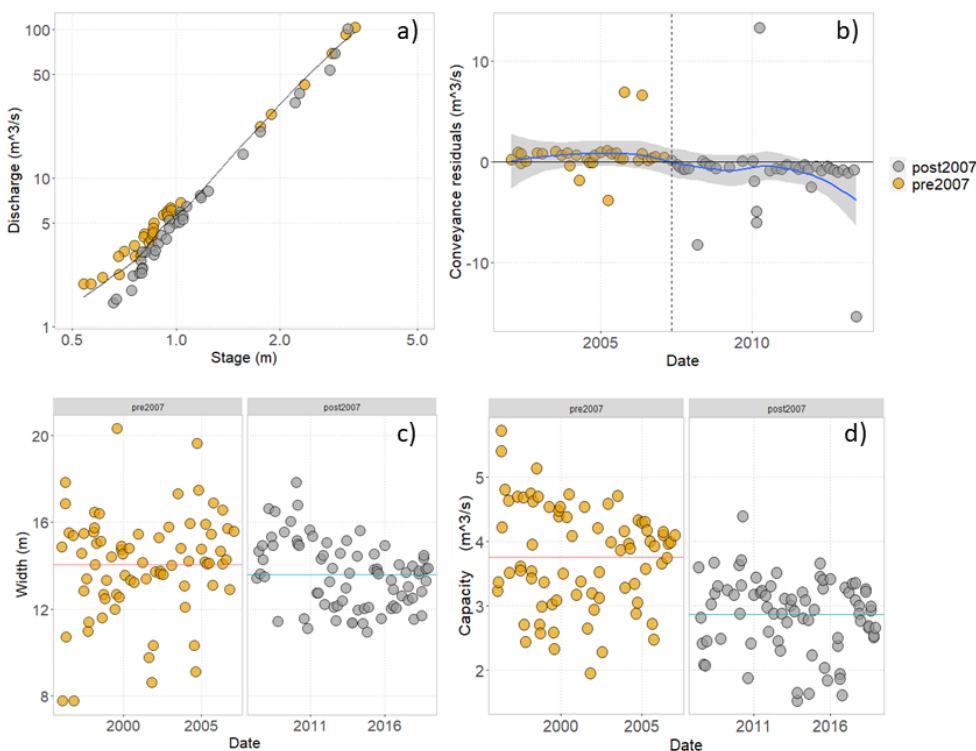
Figure 3: Illustration of the conveyance analysis for the USGS stream gage QUINNIPIAC RIVER AT WALLINGFORD (USGS station 01196500), before and after the storm of April 2007. Stage-discharge relationship fitted to flood hazard level is shown in (a), and residuals fitted to the rating curve in (b). In (b), some outlier residuals are evident, likely due to shifts in measurement locations. These points were filtered out before performing the ML training. Time series of channel widths (c) and channel capacity (d) are also shown, to highlight that possibly, the major change in residuals is due to a difference in channel depth, given a constant velocity.

2.2 Considered Predictors

To obtain information on the watershed's hydrologic and geomorphologic properties, we collected data for each gage from the GAGES II dataset (Falcone, 2011). This dataset provides for each gage landscape variables associated with watershed typical characteristics (e.g., Drainage area, Elevation, etc). These properties can be considered likely to change at a speed much slower than river discharge and localised channel measurements. Hence, we may consider these variables as 'static' in time. However, even if they are static in time, these characteristics are highly variable in space as they are spread across the CONUS, providing us with a large sample of values for the ML training.

We also investigated several extreme events from 2002 to 2013 provided by (Shen et al., 2017). We ended up with 291201 events total for the 3101 gages. The minimum and maximum numbers of events per gage varied from 1 to 520. For each available field measurement of channel properties, we consider all the storms that happened in the previous 15, 30, 90, 180, and 365 days (accounting for the lag times between each storm and the response of the river system) and calculate the

median values of the storm characteristics (as defined in Shen et al., 2017; Table 1) in that timeframe, excluding gages with less than 10 events. Therefore, for every field measurement (i.e., dot in Fig 3), we have a "typical storm" reducing the effects of small variability.

We identified three groups of drivers from these integrated data sources: atmospheric, hydrologic, and geomorphologic (Table 1). The integrated dataset provided direct and statistically derived information regarding flows and associated precipitation characteristics of each storm event.

Table 1: Variables considered in the analysis and their abbreviations. Readers should refer to Shen et al. (2017) and Falconee (2011) for a complete description of the atmospheric, hydrologic, and geomorphologic variables. Variables in bold letters are those used for ML analysis after the variable importance analysis. Please note that the description of the variables and their naming is consistent with that of the two published dataset.

VARIABLE	DESCRIPTION	Unit	VARIABLE_TYPE	Data Source
TOPWET	Topographic wetness index	ln(m)	Hydrologic	Falcone (2011)
HLR100M_SITE	Hydrologic Landscape Region (HLR) at the stream gage location.	unitless	Hydrologic	Falcone (2011)
Peak	Peak flow associated with the storm event		Hydrologic	Shen et al. (2017)
Res	Residual	unitless	Hydrologic	Estimated
IBF	Base flow index	m^3/m^3	Hydrologic	Shen et al. (2017)
Perc	Percentage of peak flow: The corresponding percentile of the peak flow in the entire flow series of the gauge	%	Hydrologic	Shen et al. (2017)
Q2	Second-order moment of the flow		Hydrologic	Shen et al. (2017)
Els	Mean water travel distance to the drainage outlet	m	Hydrologic	Shen et al. (2017)
EQ	Centroid of flow hydrograph	h	Hydrologic	Shen et al. (2017)
Vt	Normalized flow volume ~ average flow volume per unit drainage area	mm	Hydrologic	Shen et al. (2017)
HYDRO_DISTURB_INDX	Anthropogenic modification	unitless	Hydrologic	Falcone (2011)
RunoffCoef	Runoff coefficient	unitless	Hydrologic	

BFI_AVE	Base Flow Index (BFI): Base flow to total streamflow ratio, given as a percentage ranging from 0 to 100. The persistent, slowly fluctuating component of streamflow that is commonly attributed to ground-water discharge to a stream is known as base flow.	%	Hydrologic	Falcone (2011)
CLASS	Reference/non-reference class: REF = reference (least-disturbed hydrologic condition); NON-REF = not reference.	N/A	Geomorphologic	Falcone (2011)
GEOL_REEDBUSH_DOM	Dominant (highest percent of the area) geology, derived from a simplified version of Reed & Bush (2001) - Generalized Geologic Map of the Conterminous United States.	N/A	Geomorphologic	Falcone (2011)
STREAMS_KM_SQ_KM	Stream density, km of streams per watershed sq km, from NHD 100k streams	km/sq km	Geomorphologic	Falcone (2011)
STRAHLER_MAX	NHDPlus's maximum Strahler stream order in the watershed.	unitless	Geomorphologic	Falcone (2011)
MAINSTEM_SINUOUSITY	Sinuosity of mainstem streamline	unitless	Geomorphologic	Falcone (2011)
RFACT	Rainfall and Runoff factor	100s ft-tonf in/h/ac/yr	Geomorphologic	Falcone (2011)
ELEV_MEAN_M_BASIN	Mean watershed elevation (meters) from 100m National Elevation Dataset	m	Geomorphologic	Falcone (2011)
ELEV_MAX_M_BASIN	Maximum watershed elevation (meters) from 100m National Elevation Dataset	m	Geomorphologic	Falcone (2011)

ELEV_MIN_M_BASIN	Minimum watershed elevation (meters) from 100m National Elevation Dataset	m	Geomorphologic	Falcone (2011)
ELEV_MEDIAN_M_BASIN	Median watershed elevation (meters) from 100m National Elevation Dataset	m	Geomorphologic	Falcone (2011)
ELEV_STD_M_BASIN	Standard deviation of elevation (meters) across the watershed from 100m National Elevation Dataset	m	Geomorphologic	Falcone (2011)
ELEV_SITE_M	Elevation at gage location (meters) from 100m National Elevation Dataset	m	Geomorphologic	Falcone (2011)
RRMEAN	Dimensionless elevation - relief ratio, calculated as (ELEV_MEAN - ELEV_MIN)/(ELEV_MAX - ELEV_MIN).	unitless	Geomorphologic	Falcone (2011)
RRMEDIAN	Dimensionless elevation - relief ratio, calculated as (ELEV_MEDIAN - ELEV_MIN)/(ELEV_MAX - ELEV_MIN).	unitless	Geomorphologic	Falcone (2011)
SLOPE_PCT	Mean watershed slope	%	Geomorphologic	Falcone (2011)
ASPECT_DEGREES	Mean watershed aspect	degrees (0-360)	Geomorphologic	Falcone (2011)
ASPECT_NORTHNESS	Aspect "northness". Ranges from -1 to 1. A value of 1 means the watershed is facing/draining due north, and a value of -1 means the watershed is facing/draining due south	unitless	Geomorphologic	Falcone (2011)
ASPECT_EASTNESS	Aspect "eastness". Ranges from -1 to 1. A value of 1 means the watershed is facing/draining due east, and a value of -1 means the	unitless	Geomorphologic	Falcone (2011)

	watershed is facing/draining due west			
Physio	Physiographic divisions of CONUS	N/A	Geomorphologic	(Physiographic divisions of the conterminous U. S., 2023)
DRAIN_SQKM	Drainage area	km^2	Geomorphologic	Falcone (2011)
CovTrLs	Covariance of precipitation and water travel distance	mh	Atmospheric	Shen et al. (2017)
Etr	Centroid of precipitation	h2	Atmospheric	Shen et al. (2017)
VarTr	Spreadness of precipitation	h^2	Atmospheric	Shen et al. (2017)
VarLs	Variance of water travel distance	m^2	Atmospheric	Shen et al. (2017)
Vb	Base flow volume	mm	Atmospheric	Shen et al. (2017)
Vp	Precipitation volume	mm	Atmospheric	Shen et al. (2017)
Pmean	Mean Precipitation	mm/h	Atmospheric	Shen et al. (2017)
	Climate types (was not included in the ML model)		Atmospheric	

2.3. Modeling the Impact of Major Storms

The ML-based methodology developed in this study for predicting the median "Residual" is based on clusters of the gages. Using a self-organizing map (SOM) with event-specific characteristics, explained in Table 1, we developed a framework for understanding and predicting channel changes due to severe storm events. The SOM developed by (Kohonen, 1982), is one of the most popular clustering/ classification methods used in many research areas such as medical science, hydrology, and signal processing (e.g., (Zanchetta and Coulibaly, 2022; Rahmati et al., 2019). The SOM method has become a very useful prediction tool in hydrological and environmental studies because it can predict a target variable without learning any physical relationship among a collection of variables. The main advantage of the SOMs is that they allow to reduce the data dimensionality, by organizing the data into a two-dimensional array (Kohonen 1982) using topology-preserving transformations (Rahmati et al., 2019). SOMs, being a form of artificial neural network, can be thought of as a regression technique with a higher level of nonlinearity between the dependent and independent variables (Geem et al., 2007).

The proposed SOM framework (Figure 4) consisted of four phases: unsupervised clustering, supervised mapping, trained regression, 10-fold validation, and prediction. The whole procedure is described in the sub-sections below.
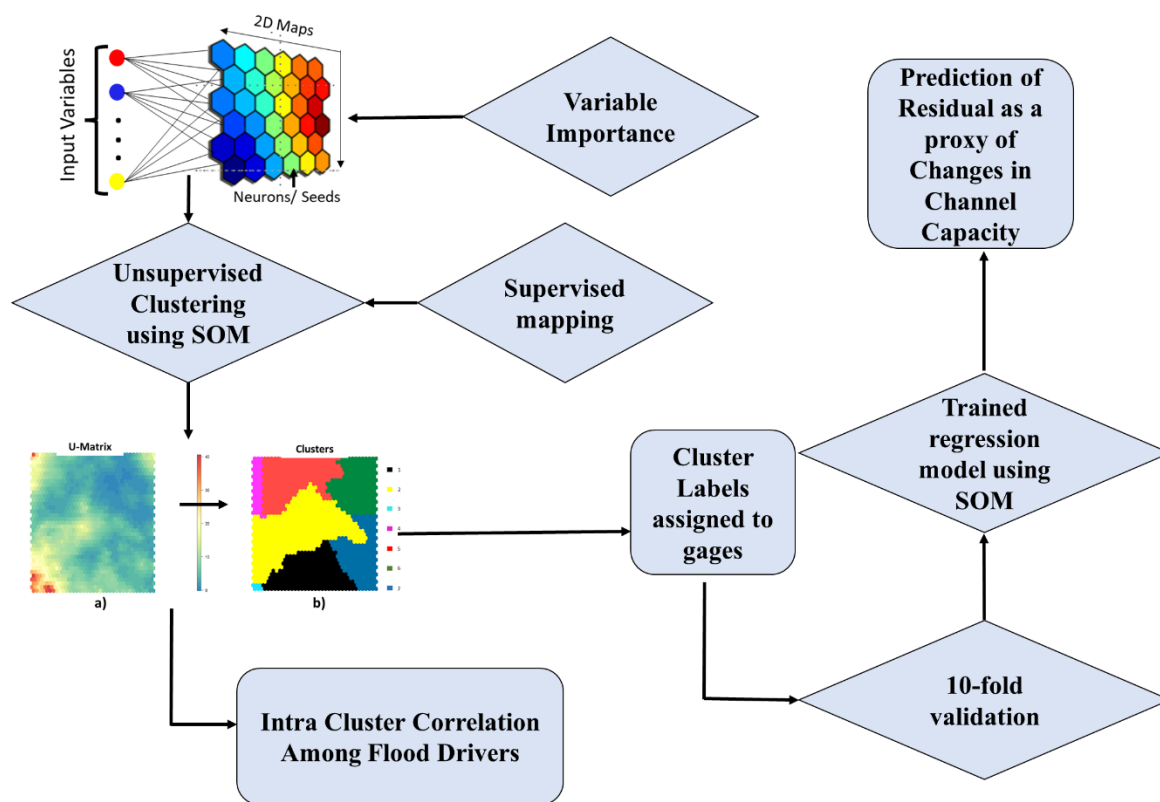
Figure 4: Schematic of the SOM framework proposed in this study.

The SOM algorithm is technically conceived for numerical datasets. This means that SOMs cannot be used to analyze categorical values. To present the categorical variables to the machine learning model selected for this study, we therefore
210 converted all the categorical values into binary digits. Each binary digit was then transformed into one feature column.

Most storm variables (except Perc- Percentage of peak flow and Percentile-Percentile corresponds to peak flow) were normalized considering the range of values available for each station. This normalization was performed to account for the influence of the watershed sizes on the various storm properties. Continuous geomorphologic and hydrologic variables, not coded in the range 0-1 (or 0-100) (aside from RRMEAN-Mean relief ratio and RRMEDIAN- Median relief ratio,
215 SLOPE_PCT- Mean watershed slope, and Aspect) were normalized considering the overall range across CONUS. The stage-discharge residuals were kept as is because they are already "relative" in value to the stage-discharge fitted at flood stage for each gage. To reduce the dataset dimensionality, and avoid collinearity, we performed a variable importance analysis using the misclassification rate (section 2.3.1).

2.3.1. Unsupervised Clustering

220   The first module used, a SOM algorithm to cluster together gages based on similar characteristics. The main objective of this step is to group together gages having similar underlying patterns of variables. The SOMs are organized in two-dimensional space where the neighbouring neurons learn similar patterns, and neurons mapped far away have dissimilar patterns (Stefanovič & Kurasova, 2011). This unsupervised mapping was performed automatically using the Kohonen package in R (Wehrens and Kruisselbrink, 2018; Wehrens and Buydens, 2007; Kohonen, 1982; Wehrens, 2019). The optimal number

225   of nodes was set at five times the square root of the number of observational data, as per Kohonen's general rule (Fytilis and Rizzo, 2013).

        Typically, SOM data clustering involves two steps: first, the data set is organized into various nodes, and then the nodes are clustered (Vesanto & Alhoniemi, 2000). Clustering speeds significantly increase when nodes are used in place of actual data. The result of the first step is that gages are grouped together in neighboring nodes if the underlining patterns of

230   variables are similar. After the SOM is trained, its U-matrix gives insight into how all the data are organized, as it displays the nodes and the distance that the weight nodes create between each weight and all its neighbors. This matrix can be used for the second step of identifying and labeling the actual clusters, through image-analysis tools (Pacheco et al., 2017, Vincent et al., 1991; Wang et al., 2010; Wu & Li, 2022). In this work, the first unsupervised clustering was accomplished by using all the data together, including the residuals in the process. Each gage was assigned a cluster number based on all the variables

235   pertaining to that location. Gages grouped in the same cluster are expected to have similar patterns of the input variables, including the residuals. For each cluster, then, we re-train the model, retaining only the gages for that cluster, to provide the most typical residual given by the combination of hydrologic, geomorphologic, and atmospheric variables.

        The most common approach is to segment the U-matrix using the watershed technique of gray-scale image processing (Costa and Netto, 1999; Vincent et al., 1991). Using a watershed analogy, the U-matrix (Figure 5) can be used to locate the

240   clusters. Large "heights" and ridges imply significant distances in the feature space, while little "valleys" represent data subsets that are similar (Ultsch and Lötsch, 2017). The segmentation is performed by flooding the valleys (similar nodes with very close distances from one to the other) until a ridge (high dissimilarity) is reached. Where the water converges, watersheds will form, having close boundaries. One cluster is represented by all the items in a segmented area or watershed. According to this approach, a minimum height threshold can be selected to define the clusters (valleys). We followed automatic thresholding

245   and set the threshold to a statistical value equal to half the standard deviation of the values. To perform this step, we applied watershed transformation and watershed-based object detection using the function "watersheds" in the R Bioconductor package (Torres-Matallana, 2016).
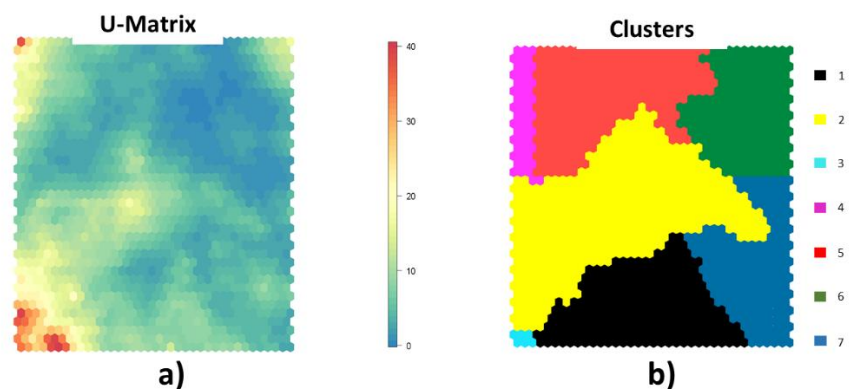
Figure 5: Example of (a) U-Matrix and (b) derived clusters. Red colors in the U-Matrix stand for significant distances in the feature
250 **space, whereas blue colors are "valleys" that group subsets of related data. The watersheds shown in (b) are collections of related**
data.

We assessed the relevance of each feature according to its misclassification rate relative to a baseline cluster assignment produced by a random permutation of feature values in order to find the most crucial features and prevent data duplication (Molnar, 2022; Breiman, 2001; Fisher et al., 2018). We preferred this approach considering that permutation

255 feature importance does not call for retraining of the model before the analysis. This approach states that a variable (feature) is "important" if changing its values results in a cluster reassignment because, in this scenario, the model primarily relies on that feature to forecast the predictors. In contrast, a feature is considered "unimportant" if changing its values has no effect on the anticipated cluster. The variable identified as important with the shuffling does not necessarily mean they have high variability among watersheds. It rather means that this variable is highly correlated with the target variable (the cluster

260 association), because shuffling its values essentially destroys any relationship between that feature and the target variable, as indicated by the decrease in the training performance. After randomly permuting the values of a feature, the model is NOT refitted to the training data. This technique has been recognized in the literature (e.g., Breiman, 2016; Fisher et al., 2018; Wei et al., 2015) and it is widely implemented in many statistic packages as well (e.g., Biecek et al., 2018, 2019; Molnar & Schratz, 2008) Please refer also to Wei et al (2015) for a review. We ran the clustering algorithm 10 times with different seeds. At each

265 run, we trained the clustering using 90% of the data and predicted the remaining 10%; and, for each run, each feature of the dataset was permuted 10 times. The permutation misclassification rate of a feature was calculated as the number of observations for which the 'permutated' cluster label differed from the original cluster assignment, divided by the number of observations given a permutation of the feature. The overall average misclassification rate iterations were interpreted as variable importance. We decided to keep only the variables producing a misclassification rate higher than the mean values. Figure 6 shows the most

270 important variables for the interval N = 365 days. This variable selection indirectly checks for collinearity by keeping only the variables that have the largest effect on the changes.
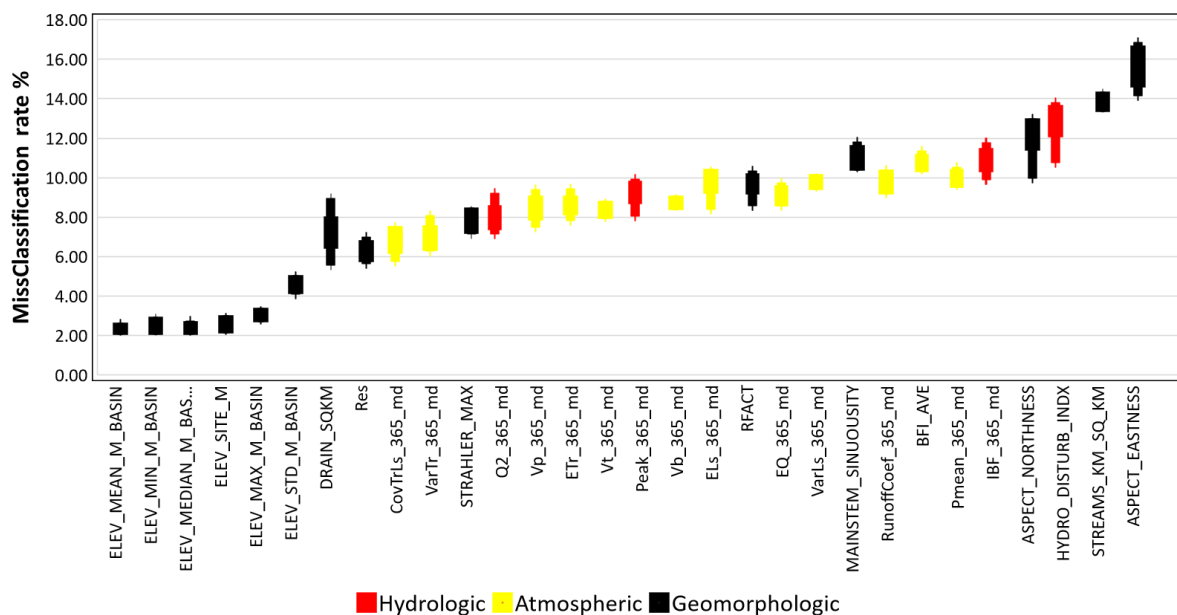
Figure 6: Selected variables based on misclassification rate (%).

275

2.3.2. Supervised Mapping and Trained Regression

Self-organizing maps (SOM) are extensively applied for clustering and visualization purposes. Nonetheless, they can be used for regression learning. (e.g., Riese & Keller, 2018, 2019). In the first step, the data (geomorphological, atmospheric, hydrologic variables, and measured residuals) are clustered together, based on patterns of variables. The resulting SOMs are

280   composed of nodes individually associated to a "weight" vector that gives a representation of the node's location in the input space. The trained map can be used to categorize new observations, by locating the cell of the SOM grid that best matches the training data (best matching unit, or BMU).

The regression algorithm of the SOM proceeds similarly to the clustering SOM algorithm. However, the regression differs for these main points: 1 Within the finalized input SOM that was created in the first stage, the BMU search is carried

285   out.; 2. For the regression instance, the weights of the supervised SOM are based only on the residuals.

Combining the unsupervised and supervised SOM allows for the selection of the BMU for each data point while also connecting the chosen best-matching unit to a particular residual estimation. In other words, each gage is mapped to a certain cluster, based on the median characteristics of the storms and the landscape. For the regression part, the data extracted from the SOM are restricted to the best matching cluster, and given the input storm and watershed properties, we can predict the

290   most likely residual.

For the supervised mapping and trained regression step, the gages were tagged to their corresponding SOM clusters. Once a cluster is defined, we aimed to determine which features were the most significantly correlated. For this, we considered the distance correlation index (dCorr) (Székely et al., 2007) to quantitatively identify the correlation of the important variables with the residuals within each cluster. The range of dCorr values, from 0 to 1, represents the dependence of two independent variables. The stronger the dependence, the closer the value is to 1, and the statistical independence of the two variables is implied by a value of zero (Sofia & Nikolopoulos, 2020). We used inverse distance correlation (1-dCorr) to measure the dissimilarity of the variables within the cluster and create organized dendrograms. The attribute distances between every pair of drivers that have been successively clustered are depicted in a dendrogram.

Having tagged the gages, we performed supervised training with them to predict the residuals based on the atmospheric, hydrologic, and geomorphologic variables. The main outcome of this part is to have a ML system able to predict the most probable residual after a storm having certain properties, for a location with specific watershed characteristics. To this point, we retrained the SOMs independently for each cluster, using only the data retrieved from the stations within that cluster. For this part, we applied an extension of Kohonen's self-organizing map algorithm, the growing self-organizing map (GSOM) (Alahakoon et al., 2000; GrowingSOM package | R Documentation, 2020, https://rdrr.io/cran/GrowingSOM/). We chose GSOM to refine the analysis and improve the prediction within each cluster. The GSOM hierarchical clustering technique enables the data analyst to locate important and unique clusters at a higher level and to focus on more precise grouping of the interesting clusters only (Alahakoon et al., 2000). The GSOM is computationally expensive, so we decided to apply it to the already clustered data. A spread factor parameterizes the GSOM. This measure can generate maps of different sizes without previous knowledge about the dataset, samples, or attributes. We set the spread factor to 0.8, as suggested by Alahakoon et al. (2000).

Finally, we trained the model by selecting 90% of the data randomly and validated its performance using the remaining 10% for each cluster. The traditional method of identifying the quality of the SOM, proposed by Kohonen, is to compute the quantization error by summing the distances between the nodes and the data points, with smaller values indicating a better fit. This method had been used successfully by many researchers, requiring minimal computation time, to compare changes across time-series images (e.g., Bação et al., 2005; Dresp et al., 2018; Wandeto and Dresp-Langley, 2019). For quality assessment, we also followed the approach used by Swenson and Grotjahn, (2019). We performed cross-validation for a particular SOM, fitting the SOM to the data first to ensure a unique cluster assignment. Then we conducted 100 trials, excluding the data used in initialization, as suggested by Swenson and Grotjahn (2019). We utilized a typical subdivision of 90-10, using 90% of the data to fit a new SOM, and predicting the cluster assignments of the remaining 10% as validation. The percentage of gages whose cross-validation cluster assignment changed from the original assignment in at least 10% of the 100 trials was calculated. We further tested the quality of the ML by evaluating the RMSE and the correlation distance between the actual residuals and the predicted ones for the validation dataset.

2.3.3. Predicting Major Storm Effects on Future Flood Hazard

325   Using the trained model (section 2.3.2), we predicted the residuals for each gaging station, based on all the variables (table 1) selected from Shen et al. (2017), Falcone (2011) and Fenneman and Johnson, 1964. We compared the predicted residual for a given storm at a given gage with the average residual measured in the most recent year. We quantified the "likelihood of change" as the percentage of times the predicted residuals showed a sudden deviation from positive to negative. This sudden deviation, as illustrated in Figure 3, can indicate a quick shift in channel conveyance in response to sediment

330   deposition, which can trigger increased flood hazard even when the flood event's return period remains unchanged (Blench 1906-1993, 1969; Lane et al., 2007; Pinter et al., 2006b, a; Stover and Montgomery, 2001).

We decided to approach this change in terms of how often a gage is predicted to change after a storm. We also compared the average residuals predicted from all the storms for a given gage with the confidence interval of the current stage-discharge relationship, calculating the ratio between the mean prediction and the lower bound of the confidence interval for those stations

335   with predictions showing a deviation from positive to negative. If a gage had a positive residual, and the predicted one after flood was negative, and outside the confidence bound of the fitted curve, we labelled this gage at risk. The greater this value, the more likely the changes would be outside the range of the current stage-discharge error.

3. Results Analysis

3.1. Variable Importance

340   Figure 6 demonstrates the outcome of the variable importance. Based on the results shown in Figure 6, we found that the same variables were always important for all intervals. analysis. Table 1 shows all the selected variables in bold for N = 365. In this case, out of a total of 40 variables we have selected 30 based on the misclassification rate (%). Of the selected variables 15 were geomorphologic variables, followed by 10 atmospheric variables and 5 hydrologic variables. This confirmed the importance of the geomorphology of the watersheds. While this result on channel changes was expected, it further

345   highlighted the critical significance of geomorphology for the dynamics of flood hazards, as most of the geomorphologic parameters were important for the prediction of the residuals. The most important were the variables Aspect (ASPECT_NORTHNESS, ASPECT_EASTNESS), and stream density (STREAMS_KM_SQ_KM). The significance of "Aspect" attributes can be understood in terms of the various runoff and soil loss yields that can result from changes in slope properties. For example, hillslopes on opposite aspects tend to have various degrees of erosion and degradation due to

350   (compound) differences in soil characteristics, water availability and vegetation development (Kutiel et al. 1998, Nadal-Romero et al. 2014).

Another essential characteristic of the Earth's surface that regulates mass and water movement on the landscape is drainage density (Clubb et al., 2016), which is correlated with subsurface permeability (Luo et al., 2016). The control these factors exert on sediment production and delivery and soil permeability may explain the importance of these variables to post-

355   storm changes in river conveyance.

The most important hydrologic variable was HYDRO_DISTURB_INDX, which explains the condition of the watershed, whether it is anthropogenically modified or natural. Ahrendt et al. (2022) confirmed that channel regulation is important to conveyance changes. Similarly, the construction of dikes, bridges, dams, meander cutoffs, channel constriction by wing dikes, groynes, and other engineering projects can alter channel conveyance within rivers and the characteristics of

360 their floodplains. (Bormann et al., 2011; Pinter et al., 2006b, a) The importance of this variable in the model highlighted the potential interaction of extreme storm events that generate high sediment deposition with the effects of flow regulation structures.

3.2. Evaluation of SOMs accuracy

The quantization error (Table 2) provided a measure of the accuracy of SOMs. The quantization error reported a

365 higher accuracy as the number of training samples increased (increasing the number of days, resulting in more channel measurement and flood properties for each training sample). Homogeneous areas in the U-Matrix became more evident (Figure 7) as the quantization error diminished (Table 2). As Table 2 indicates, the 365 days interval had the best quality, as represented by the lowest quantization error. For this reason, the following sections will present an investigation of the maps produced with this interval. Table 2 also shows the SOM quality in terms of distance to the closest units of the SOMs trained for each

370 cluster. The results suggest that the retraining of the individual cluster using GSOM improved the prediction quality of the SOM significantly.

Table 2 also represents the correlation distance and RMSE between the measured and predicted residuals for each cluster of the validation datasets. The average correlation was close to 1 for all N values, suggesting the performance of the SOM model was satisfactory. The average RMSE was close to 0, which was also an indication of the quality assurance of the

375 SOM model. Both the unsupervised correlation distances and the average correlation showed the best results for N- 365 days. The RMSE diminished with the increase in the interval.
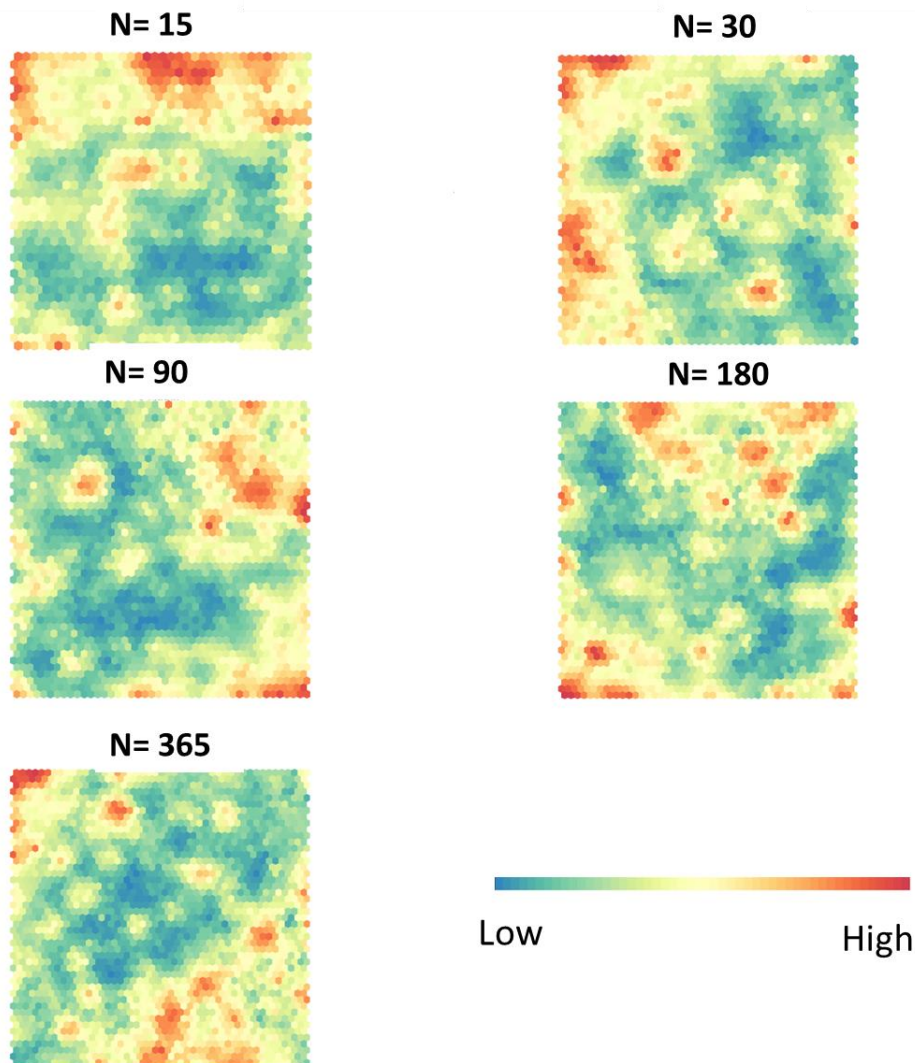
Figure 7: U-Matrix for different intervals (N days). The red colors represent large distances in the feature space, while the blue colors represent "valleys "grouping subsets of similar data.

380   **Table 2: Accuracy assessment parameters of the ML analysis. This table reports the average correlation and RMSE for the different intervals.**

Interval (days)	Avg. Corr. (10-fold)	Avg. RMSE (m) (10-fold)
15	0.81	0.13

30	0.84	0.14
90	0.80	0.13
180	0.80	0.09
365	**0.86**	**0.09**

Figure 8 presents the results of the unsupervised clustering for N = 365 for the variables used. In the figure, the contrast between high (red) and low (blue) value areas emphasizes the spatial patterns of the various parameters we investigated. Based on this clustering, a combined U-Matrix is produced (discussed in Figure 7) and a cluster label is assigned to each gage. Gages with similar characteristics presented by the variables are tagged with the same cluster number. We have got 12 clusters of gages. We have plotted the clusters individually on a map showing how they spread across different physiographic regions and climate zones in Figure A1 in Appendix A. Clustering does not have a geographical meaning, rather gages behave more consistently between adjacent clusters than non-adjacent clusters, but this does not necessarily follow the spatial proximity of the gages. This is reflected in the spatial spread of the different clusters of gages in Figure A1.

If we focus on the SOM of "Res", we can see that the nodes on the righthand side of the SOM seem to be associated with high values of the residuals (Figure 8). Nevertheless, a small cluster of high residuals is seen in the upper lefthand corner. At the global level, this highlights a lack of regional synchrony in stage-discharge shifts at the yearly scale. Pfeiffer et al., (2019) reported similar findings on the decadal scale.

Based on the visual interpretation of the unsupervised SOMs, taking the atmospheric, hydrologic, and current geomorphologic conditions as single independent drivers is not sufficient to predict the magnitude of the shift in stage-discharge at the flood stage. This suggests the co-occurring fluctuations in the various parameters, rather than variation in a single peak parameter, are the primary drivers of change in flood hazard at the continental scale.
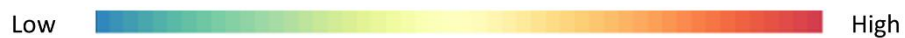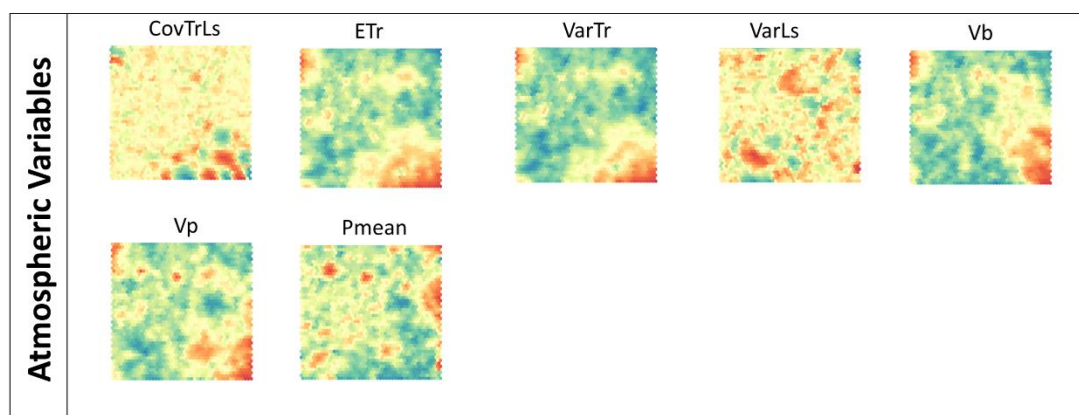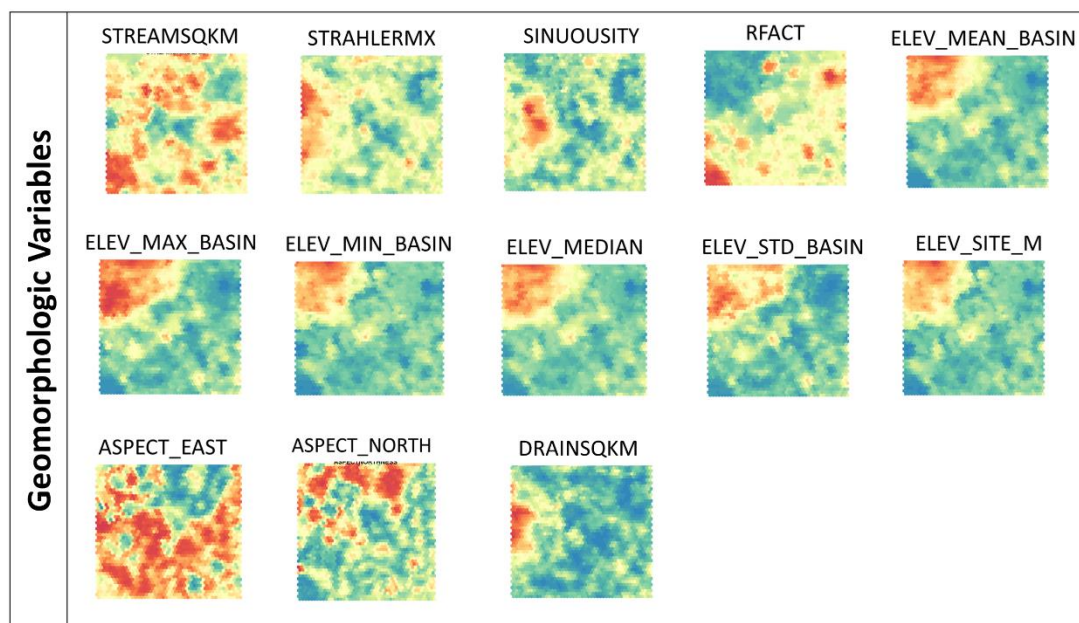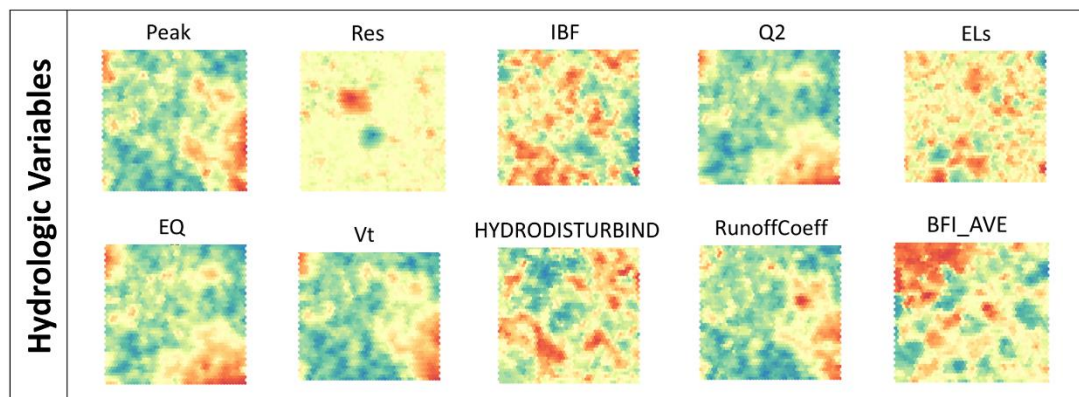
Figure 8: Individual SOMs of all the flood drivers for N= 365. Similar to the U-Matrix the red colors represent large distances in the feature space, while blue colors represent "valleys "grouping subsets of similar data.

Visually, the SOMs in Figure 8 highlight the co-oscillation of hydrologic and geomorphologic variables as a standard
405 component of watershed behaviour. Drainage area (DA) and discharge/peak flow (Peak), for example, are positively correlated, with a cluster of high values in the bottom part of the SOMs. We can see that, other hydrologic variables like ELS (Mean water travel distance to the drainage outlet), EQ (Centroid of flow hydrograph), Q2 (Second-order moment of the flow), Vp (Precipitation volume), Vt (average flow volume per unit drainage area), and VaTr (Spreadness of precipitation), have similar patterns. The centroid of precipitation (EQ) and hydrograph (ETr) appear to be highly correlated. Some specific co-
410 oscillations of variables are evident in multiple regions. Percentage (Perc) and percentile (Percentile) of peak flow show the highest values spread across the SOM nodes. This is consistent with the fact that along with the drainage area, the duration and spatial pattern of rainfall are responsible for the variability in lag time and basin response (Granato, n.d.; Woods and Sivapalan, 1999). The correlation among Drainage area (DA), peak discharge (Peak), and Mean water travel distance to the drainage outlet (Els) is evident for various clusters, as is the correlation between Normalized flow volume (Vt) and Baseflow
415 (Vb). This is not surprising, considering that the basin size is generally the most important basin characteristic in determining the amount and timing of surface runoff at the outlet (Gupta and Dawdy, 1995). And the relationship between flood flow quantiles and drainage area is expressed by power-law equations (Villarini and Smith, 2010). It also confirms how catchments with larger drainage areas display higher values of specific discharge and how morphodynamic properties (including low flows) tend to cluster with drainage network characteristics and scaling properties (Saghafian, 2005; Reis, 2006; Sofia and
420 Nikolopoulos, 2020b). Further cross-cluster variability occurs with some atmospheric and hydrologic variables, namely the Centroid of precipitation (ETr), Centroid of flow hydrograph (EQ), and Spreadness of precipitation (VarTr). All the previously mentioned variables present their co-occurring peaks in Cluster 6 (the Upper Mississippi and Missouri region), which is in line with the fact that for this area (and cluster), snowmelt, rain on snow, or rainfall can cause major flooding.

3.3. ML Advantages and Limitations

425 A critical aspect of the approach is that randomness is introduced every time feature permutation is applied (Molnar, 2022). Such randomness might not be representative of a real physical process. When repeating the permutation, the results may vary considerably (Molnar, 2022). To increase robustness and stabilize the measure, we repeated the permutation and averaged the importance measures over the various reiterations.

A further aspect to consider is that if the features are in reality correlated, permutation might introduce unrealistic
430 (uncorrelated) data, determining an unlikely combination of the parameters. This issue is more evident if real-world variables are directly or inversely correlated; by shuffling one of the features, we may be creating new unlikely or physically impossible instances. Therefore, as Molnar (2022) suggested, we may be potentially looking into a decrease in the model performance only due to values that we would never observe in the real world.

We should point out that channel conveyance change is known to vary spatially across a region and strongly correlates
435 with climate variations and landscape properties. The feature permutation randomness for our study case was, however, counteracted by the two main features of SOMs: (1) SOMs tend to preserve neighbourhoods, which results in spatial clusters of comparable patterns in the output space; and (2) SOMs 'adapt', so that the winner neuron and its neighbours are changed to make the weight vectors more similar to the input. Due to these two features, random 'unrealistic' gages would likely end up grouped into a single neuron, whereas 'real' data are mapped into different neurons. During the BMU phase, therefore,
440 actual gages are mapped to the most similar neuron, likely excluding randomness. Besides that, using multiple attributes, such as combined atmospheric, hydrologic, and geomorphologic variables, can improve the pattern generated by the SOM. In our approach, the variable importance did not change, considering the various N intervals used to group storm properties. The high correlation between estimated residuals and measured ones during the 10-fold validation confirmed the accuracy of the model.

Careful interpretations that explain how and why channel conveyance changes happen as they do are essential to
445 guiding reliable predictions of river conveyance behaviour and evolution. Another aspect to consider, as for any ML approach, is that SOMs are stochastic, as there are no physical constraints in their prediction. The use of randomness as a feature in the SOM analysis exerts confidence in the results mainly when the results are agreeable with the theoretical aspect of the variables. We suggest referring to Brierley et al., (2021) for a recent review of ML limitations in geomorphology in general.

3.4. Changes in Flood Vulnerability after Major Floods

450 We have interpreted the changes in flood vulnerability at each gage based on changes in predicted residuals. Figure 9a shows the groups of gages representing different percentages of "likelihood of change." If the reported value is <10%, for example, the predicted residuals for those gages show a sudden change from negative to positive in less than 10% of storms. The higher the percentages are, the more likely we expect a drastic reduction of channel capacity after a large storm. Comparing with the literature (Slater et al., 2015), we can see that, in our study, the locations with the highest likelihood of change
455 coincided with those with significant channel capacity and net changes in flood hazard frequency. While the post-storm change was not as widespread as the effects highlighted by Slater et al. (2015), this was expected, as we were analysing post-storm effects and not considering the persistence in time of these changes at this stage. Also, a higher rate of change (high percentage) might be representative of very dynamic rivers, whose changes are likely to smooth out in time. On the other hand, rivers changing less frequently might be witnessing changes with a magnitude sufficient to last longer. This fact should be addressed
460 carefully. Another thing to consider is that, because USGS gages are operationally placed at stable locations, our analysis, as well as other works (e.g., Li et al., 2020; Slater et al., 2015), does not capture the full range of the consequences of conveyance changes.

Nonetheless, our results highlighted how substantial changes had occurred even for these locations. When we focused on the amount of change relative to the current confidence bound of the stage-discharge (Figure. 9b), we could see that the
465 magnitude of change was higher for gages that changed less frequently. The northwestern part of CONUS, where Slater et al. (2015) highlighted clustering of increase in hazard due to consistent channel capacity changes with clusters of gages for which

23

we predicted negative residuals outside the confidence bound of the stage-discharge relationship. For the Northeast, on the other hand, our model predicted high-magnitude changes for areas identified by Slater et al. (2015) as areas significantly impacted by flow frequency effects. It is known that existing stage-discharge relationships present uncertainty in estimating

470 the discharge because of the variation in the individual measurements from which the estimation is derived. Our model highlighted that the post-storm increased change lay outside the range of acceptable uncertainty at many gages. As Figure. 9b shows, this change was as widespread as the effects highlighted by Slater et al. (2015) for total positive changes in flow hazard frequency (FHF). For gages in both this work and Slater's, the total FHF increased logarithmically, as our predicted changes lay further in the negative domain, outside the lower confidence bound.

475
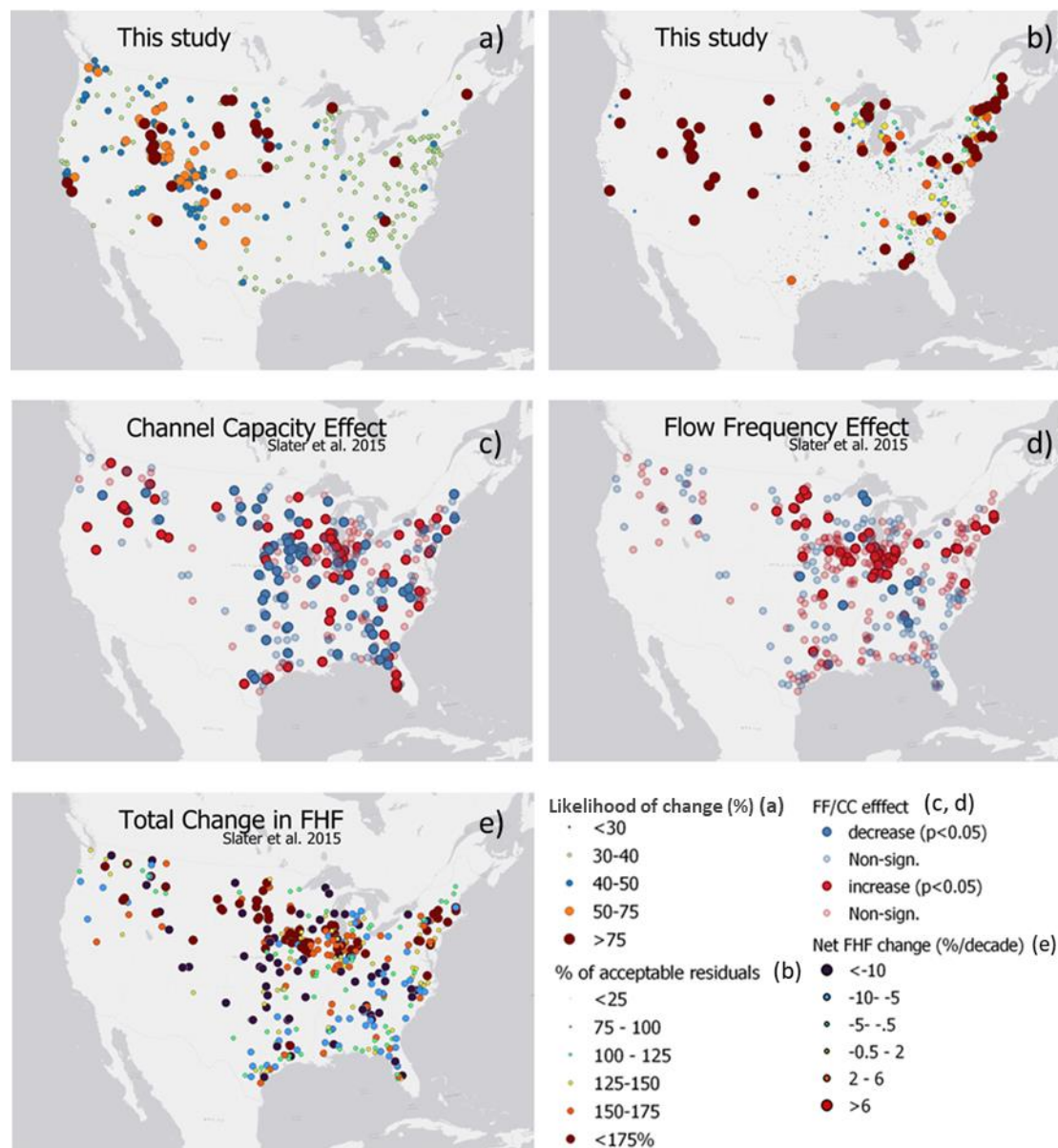
Figure 9: Predicted changes as compared to the results of Slater et al. (2015) showing Channel Capacity (CC) and Flow Frequency (FF) effects on flood hazard frequency (FHF). In (a) "Likelihood of change"- the percentage represents the number of times the model predicts a residual change from positive to negative after a major flood (for N = 365); in (b) the panel shows the ratio between average prediction and lower 95% confidence bound of the current stage-discharge relationship for the stations showing a drastic change positive to negative. In (a, b) gages with small variations from this study have been reduced for clarity. Panel (c,d, and e) are results from Slater et al. 2015.

From the predicted results of the channel changes at the gage level, we next analysed which locations were more prone to changes based on the number of gages with predicted changes within each physiographic region and climate type (Figure 10). Among the physiographic regions (Figure 10a), the Laurentian uplands and intermontane plateaus had the most

changes (75% of all gages in this region). Rocky Mountain and Pacific mountain systems followed the trend with the second most changes (50–75%). The changes in the <10% of the gages resided in the Interior Highlands, Atlantic Plains, and Appalachian highlands.

490   The Appalachian Highlands regions are mountainous. In contrast, the interior plains are mostly flat agricultural lands whose river system consists of the upper Mississippi River, the Ohio River, parts of the Great Lakes, and small wetlands. This region has very dynamic hydrology, with very cold winters and hot summers. Snowmelt in the spring and heavy precipitation in the summer and winter result in big floods. Naturally, this can potentially lead to changes in the river reaches. While the Atlantic Plain is also relatively flat, it covers the Mississippi Delta, the Gulf of Mexico, and the Atlantic seaboard in the East (see Figure 2). The interaction with the ocean gives this region the most complex sediment activity. The coastal plain is also

495 influenced frequently by tropical storms and cyclones, which results in a lot of sediment activity. The literature (Bracken and Croke, 2007; Kalantari et al., 2019; Croke et al., 2013; Sofia and Nikolopoulos, 2020a; Wohl et al., 2019) has highlighted sediment connectivity as a potentially critical factor in flood hazards, being linked simultaneously to changes in channel characteristics and shifts in decadal trends in flood hazard, independent of scale. In addition, for these regions, and in the eastern United States more generally, peak flows are highly variable (Villarini & Smith, 2010), and tropical cyclones affect

500 the distribution of extremes. All these characteristics contribute to the presence of very dynamic rivers, which, as confirmed by our model, quickly react to extreme events, adjusting their geometry and possibly altering future flood hazards.

     We made the same comparison for the climate types (Figure 10b). We detected high predicted variability mainly in hot and humid climate regions, while cold and dry regions showed minimal changes. Humid Continental climate (Dsb, Dfa, Dfb) led with the highest variability (>75% of the gages resided in these climate regions). The gages with 50–75% channel

505 changes were in the Tundra Climate (ET) and Warm Summer Mediterranean Climate (Csb). Gages with the least changes (<10%) were located in Humid Continental Hot Summers with Dry Winters (Dwa), Continental Subarctic-Cold Dry Summer (Dsc), Cold Desert Climate (Wk), and Hot Semi-Arid Climate (BSh). These climate zones are mostly dry either year-round or seasonally. Our findings confirmed that the impact of major storms on rivers depends on both underlying long-term climate signatures (Chen et al., 2019; Stark et al., 2010) and short-term (year-to-year) climate variability (Slater et al., 2019). For many

510 river systems, coarse sediment mobilization and transportation rates are controlled by regional climate (Anderson and Konrad, 2019). Climate variability is projected to trigger a chain reaction of geomorphic responses, including changes in downstream channel properties. Other studies focusing on long-term changes rather than extreme events have shown how decadal-scale changes in river morphology may be accounted for as a downstream propagating channel reaction to regional climate variability, which is frequently accompanied by cyclical changes in channel geometry and conveyance. (Scorpio et al., 2015;

515 Slater et al., 2019). The joint contribution of physiographic regions (as a proxy for sediment characteristics) and climate properties confirms the nonlinearity of system response and the coupled impacts of climate conditions and sediment connectivity. (Lane et al., 2007).
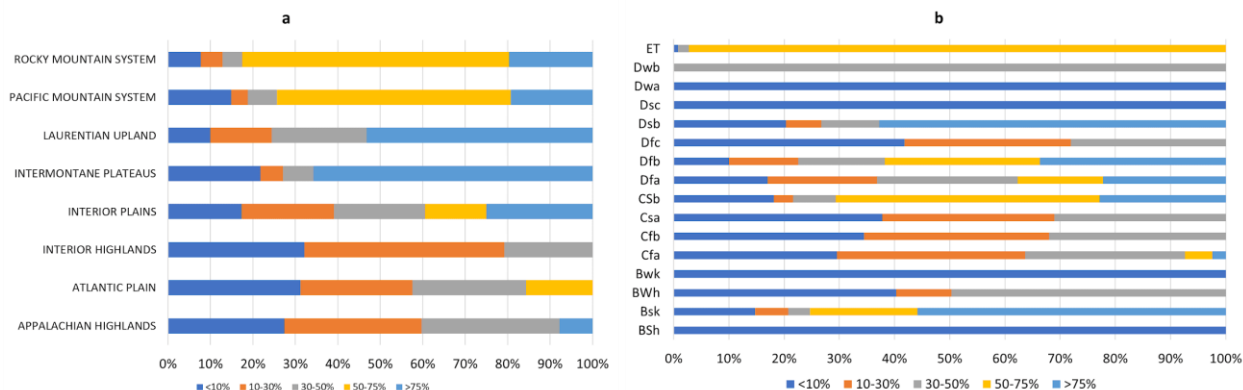
Figure 10: Percentages of gages presenting changes in channel capacity in different (a) physiographic regions and (b) climate types.

3.5. Variables Associated with Flood Vulnerability and Channel Changes

Focusing on the changes in the stage-discharge relationship residuals (Res), we next investigated the correlation between predicted and measured residuals on the one hand and other variables on the other (Figure 11, Table 3). For the proposed ML framework, the training was unsupervised. In general, the predicted and measured residuals were highly correlated, validating the SOM performance. Table 3 summarizes the correlations among the considered predictors in Figure 11 for N = 365 days. It presents the analysis of the group of variables based on the dendrogram branches for different likelihood of change levels (e.g., 0–10%, 10–30%, and 30–50%). This section discusses the correlations for the 30–50% category as an example; the other two categories showed similar outcomes. We do not have more than 50% here in the table because the highest percentage of gages that showed sudden change was 30-50%. In Table 3, level 1 shows the group of variables highly correlated to each other and with residuals. Level 2 shows variables that are highly correlated to each other but related to a lesser degree to the variables in Level 1.

In level 1, the physiography of the basins is represented by the following variables- ELEV_* EQ, Q2, and ETR (Please see table 1 for explanation), which are correlated with all the other variables. The physiography of the basin deeply controls the complex land-atmospheric interactions and storm types resulting in rainfall runoff. Thus, this is no surprise that physiography alone is highly correlated to all other (hydrologic, geomorphologic, and atmospheric) variables used in this study. This highlights the importance of basin attributes in prompting stage-discharge variability at gage locations.

EQ-Centroid of the flow hydrograph and Q2-Second-order moment of the flow are also in group 1 of level 1. Investigations of the influence of the flow stage on channel conveyance often focus on the impacts of peak or minimum bankful discharges. Recession rates matter in sediment delivery, however, as highlighted in the literature (e.g., Hassan et al., 2006), and these two properties appear to be highly correlated with the impact of large storms on flood hazards. The findings of this study provide needed insight, and managers could use the results to determine the flow hydrograph shapes that potentially alter short-term flood hazards. Such knowledge is necessary for the design of river infrastructure.

The next variable is the ETR-Centroid of precipitation. Many papers in literature (e.g., (Borga et al., 2008; Woods and Sivapalan, 1999; Woods, 1999; Smith et al., 2004, 2005, 2002; Zhang et al., 2001)highlighted the relationship between the centroid of precipitation and runoff production. Most works showed that, for example, the position of the storm centroid relative to the watershed outlet is an important driver of runoff: storms having a precipitation centroid positioned in the central portion of the watershed tend to produce a higher runoff than storms having a centroid near the outlet or the head of the watershed. This is in line with the fact that rainfall runoff spatial variability influences flash flood severity relative to basin physiography and climatology. Flash flood severity, or flashiness, as defined by Saharia et al., (2017), assesses a basin's capacity to produce severe floods by considering both the volume and timing of a flood. It is, therefore, not unexpected that the centroid of precipitation appears to be highly correlated with the shifts in residuals.

In level 2, Residuals (Res) are shown to be correlated with different variables. A noticeable pattern is group 1 contains mostly hydrologic variables, while group 2 contains atmospheric variables. In group 1, the residuals (Res) belong to the tree containing the variables RFACT (Rainfall and Runoff factor), HYDRO_DISTURB_INDX (Anthropogenic modification), STREAMS_KM_SQ_KM (Stream density), BFI_AVE (Base Flow Index), ASPECT_NORTHNESS, ASPECT_EASTNESS, STRAHLER_MAX (Maximum Strahler stream order in the watershed), MAINSTEM_SINUOUSITY (Sinuosity), DRAIN_SQKM (Drainage area), Peak (Peak flow), and CovtrLs (Covariance of precipitation and water travel distance) (level 2 in table 3).

RFACT- Rainfall runoff factor, directly affects rainfall runoff influencing the channel changes. HYDRO_DISTURB_INDX (see section 3.1) represents the channel condition, whether the channel is altered by manmade construction or not. Channel conveyance changes are highly affected by engineered constructions (Bormann et al., 2011; Pinter et al., 2006a, b), and the correlation result from our analysis supports these findings, indicating that human modifications are an important element to be considered when analysing flood hazard changes. As mentioned previously, ASPECT_NORTHNESS and ASPECT_EASTNESS influence the daily cycle of solar radiation affecting the temperature, humidity, and soil moisture (Desta et al., 2004) that control the vegetation and, hence, the sediment movement of the floodplain. The variability of these factors can, therefore, affect sediment production and movement, with consequences for flood hazard changes.

A group of highly connected elements comprises a series of drainage properties (STREAMS_KM_SQ_KM, STRAHLER_MAX, MAINSTEM_SINUOUSITY, DRAIN_SQKM) that modulate the way precipitation is routed through the basin and directly affect flood properties. Peak flows and flooding tend to reduce as network sinuosity increases (Seo and Schmidt, 2012; Seo et al., 2015; Saco and Kumar, 2002). Watersheds presenting a more homogeneous flow path length generally show higher peak flows and shorter time to peak, as well as duration (Saco & Kumar, 2002). Also, the fractal dimension of the river network is inversely related to flood frequency (Zhang et al., 2015). Our model suggests these properties are highly correlated with residual changes and indirectly linked to post-storm modifications of flood hazards. Lastly, the Base Flow Index and Peak discharge are directly related to runoff and, thus, channel conveyance changes. Because the base flow index and Peak discharge define how much volume of water is in the channel. If the volume exceeds the channel conveyance

capacity the channel is expected to change. This finding also supports the critical role of the minimal flood (baseflows) and bankfull discharge in river morphology. The variability of baseflow is also caused by groundwater recharge, which is a direct product of geologic and physiographic variations.

580   In level 2, group 2, the tree contains Pmean (Mean Precipitation), ELS (Mean water travel distance to the drainage outlet), EQ (Centroid of flow hydrograph), Q2 (Second-order moment of the flow), Vp (Precipitation volume), Vt (average flow volume per unit drainage area), and VaTr (Spreadness of precipitation), VarLs (Variance of water travel distance), Vb (Base flow volume), and RunoffCoef (Runoff coefficient). These are mostly related to rainfall properties. While they are important fingerprints for the attribution of regional flood changes, these variables are related to changes in flood hazard to a lesser degree than physiography and flow properties.

585   Overall, the results of our analysis highlight how the impacts of a storm event on channel properties and flood hazards are highly correlated with flow characteristics and a region's geophysical signature.
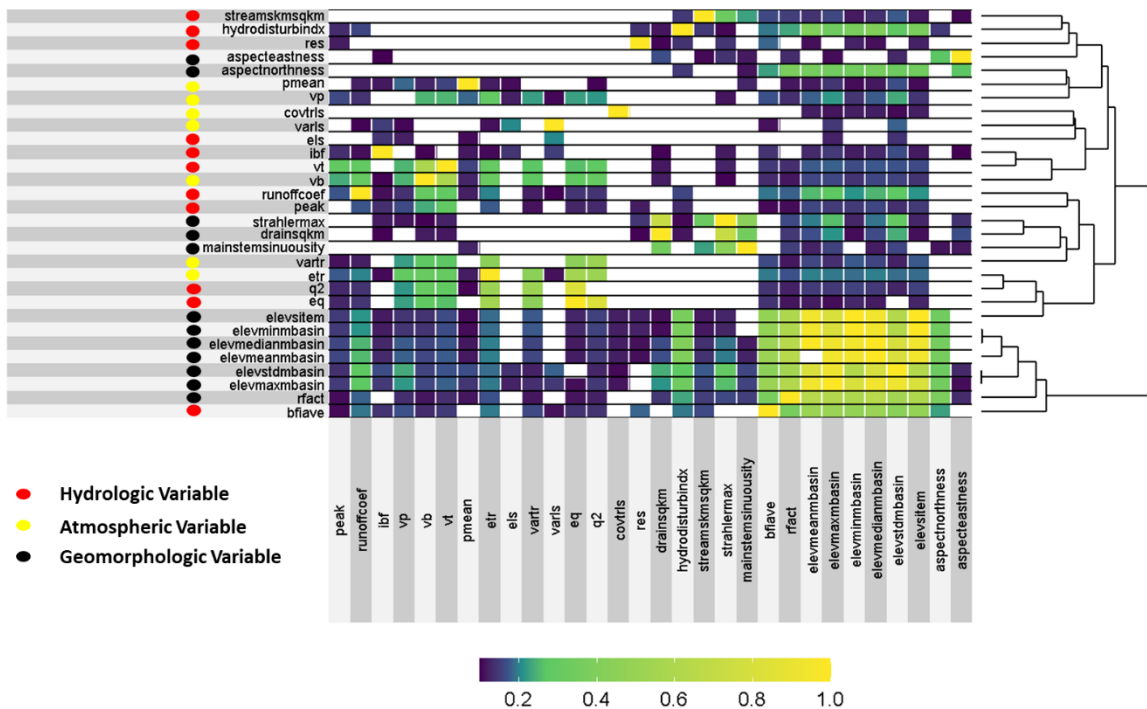
Figure 11: Example of intercorrelation among the flood drivers for N = 365 days for the likelihood of change between 30 and 50%. The white color signifies that there is no correlation between those variables. The color bar from blue to yellow shows high to low
590   **correlations.**

Table 3: Highly correlated variable groups for different percentages (%) of the "likelihood of change" from the interpretation of the dendrogram in Figure 11. Levels in the table represent the main branches of the dendrograms and groups represent the sub-branches under the main levels.

29

	0-10%	10-30%	30-50%
Variable groups	**Level1:** Group1: ELEV_MEAN_M_BASIN, ELEV_MAX_M_BASIN, ELEV_MIN_M_BASIN, ELEV_MEDIAN_M_BASIN, ELEV_STD_M_BASIN, ELEV_SITE_M, RFACT Group 2: All the other variables	**Level1:** Group1: ELEV_MEAN_M_BASIN, ELEV_MAX_M_BASIN, ELEV_MIN_M_BASIN, ELEV_MEDIAN_M_BASIN, ELEV_STD_M_BASIN, ELEV_SITE_M, EQ, Q2 Group 2: All the other variables	**Level1:** Group1: ELEV_MEAN_M_BASIN, ELEV_MAX_M_BASIN, ELEV_MIN_M_BASIN, ELEV_MEDIAN_M_BASIN, ELEV_STD_M_BASIN, ELEV_SITE_M, EQ, Q2, ETR Group 2: All the other variables
	Level 2: Group1: HYDRO_DISTURB_INDX, STREAMS_KM_SQ_KM, Res, ASPECT_NORTHNESS, ASPECT_EASTNESS, Vp, Pmean,CovtrLs, Vb, Vt, Els, IBF, VarLs Group 2: EQ, ETR, Q2, VarTr, RunoffCoef, Peak, STRAHLER_MAX, MAINSTEM_SINUOUSITY, DRAIN_SQKM	**Level 2:** Group1: RFACT, HYDRO_DISTURB_INDX, STREAMS_KM_SQ_KM, BFI_AVE, Res, ASPECT_NORTHNESS ASPECT_EASTNESS Pmean, Els, IBF, VarLs Group 2: Vp, CovtrLs, IBF, Vb, Vt, ETR, VarTr, RunoffCoef, Peak, STRAHLER_MAX, MAINSTEM_SINUOUSITY, DRAIN_SQKM	**Level 2:** Group1: RFACT, HYDRO_DISTURB_INDX, STREAMS_KM_SQ_KM, BFI_AVE, Res, ASPECT_NORTHNESS ASPECT_EASTNESS STRAHLER_MAX, MAINSTEM_SINUOUSITY, DRAIN_SQKM, IBF, Peak, CovtrLs Group 2: Pmean, Els, VarLs, Vp, Vb, Vt, VarTr, RunoffCoef

4. Conclusions

595   The variability of geomorphologic processes and future flood patterns can only be understood by evaluating all the critical flood drivers responsible. In this era of extreme events and rapidly changing landscapes, accurate flood vulnerability assessment is paramount. Atmospheric, hydrologic, and geomorphologic parameters constitute both the main driving force behind and the detector of changes resulting from an extreme event. This study focused on the impact of extreme flood events on future flood hazards by exploring the channel changes following them. We utilized the interdependencies of the

600   atmospheric, hydrologic, and geomorphologic flood drivers to gain an understanding of the impact of extreme events on channel capacity.

        Our results confirm existing knowledge of watershed hydrology and further strengthen the compound importance of climate and geomorphology as drivers of changes in flood hazards. The sequential processes during and after a big flood event can only be understood by considering the contribution of all the flood drivers together. The results show how the variables of

605   different flood drivers are interrelated and can create effects that are more adverse together.

         Channel conveyance is often regarded as stationary in flood hazard modelling, and is acknowledged as one of the most important sources of uncertainty. Our research reveals that the assumption of channel stationarity may result in either over or under-prediction of the river discharge and eventually over/under-estimation of flood hazard. These models incorrectly feed flood control planning procedures, which raises the level of uncertainty in evacuation and rescue operations. Additionally,

610   flood insurance plans created using these models' results are likewise incorrect. Furthermore, if engineering designs are based on data collected prior to periods when major flood events have lowered channel conveyance, there is a risk that surveyed channel dimensions and flood conveyance will be overestimated in the long run.

        The proposed ML model allows us to identify dynamic rivers more prone to changes in the stage-discharge relationship after major flood events. The proposed model does not account for the persistence of changes; that being said, the

615   results highlight the risk of immediate change after a large storm. For rivers more prone to changes, periodic revision of flood frequency statistics is advisable for hazard assessments to keep pace with altered conditions.

        This study considered a limited set of drivers, excluding, for example, human activities in the watersheds and vegetation properties. In response to increased flow, we do not anticipate channel conveyance to rise consistently everywhere. The intricate interaction of dynamic anthropogenic, climatic factors and their consequential processes within each basin, are

620   expected to be evident in the fluvial changes. Hence, future channel changes, sediment connectivity, Land-Use and Land-Cover Change an anthropogenic factors could also be included to retrain the model to produce changes in the stage-discharge relationship at the flood stage and potentially create scope for future prediction of channel changes due to extreme events.

Data Sources:

- Flood stage values are provided by the US National Weather Service (National Oceanic and Atmospheric Administration, 2021).
630
- Historical mean daily streamflow records are stored by the US Geological Survey (USGS) and made publicly available online (U.S. Geological Survey, 2021a).
- The flood event database used in the study was generated by Shen et al. (2017).
- Historical field measurements of channel properties are made publicly available online by the USGS (U.S. Geological Survey, 2021b).

635 **References**

Ahearn, E. A.: Flood of April 2007 and Flood-Frequency Estimates at Streamflow-Gaging Stations in Western Connecticut: U.S. Geological Survey Scientific Investigations Report 2009-5108, 40, 2009.

Ahrendt, S., Horner-Devine, A. R., Collins, B. D., Morgan, J. A., and Istanbulluoglu, E.: Channel Conveyance Variability can Influence Flood Risk as Much as Streamflow Variability in Western Washington State, Water Resour Res, 58,
640 e2021WR031890, https://doi.org/10.1029/2021WR031890, 2022.

Alahakoon, D., Halgamuge, S. K., and Srinivasan, B.: Dynamic self-organizing maps with controlled growth for knowledge discovery, IEEE Trans Neural Netw, 11, 601–614, https://doi.org/10.1109/72.846732, 2000.

Alfieri, L., Feyen, L., Dottori, F., and Bianchi, A.: Ensemble flood risk assessment in Europe under high end climate scenarios, Global Environmental Change, 35, 199–212, https://doi.org/10.1016/j.gloenvcha.2015.09.004, 2015.

645 Anderson, S. W. and Konrad, C. P.: Downstream-Propagating Channel Responses to Decadal-Scale Climate Variability in a Glaciated River Basin, J Geophys Res Earth Surf, 124, 902–919, https://doi.org/10.1029/2018JF004734, 2019.

GrowingSOM package | R Documentation: https://www.rdocumentation.org/packages/GrowingSOM/versions/0.1.1, last access: 12 July 2020.

Bação, F., Lobo, V., and Painho, M.: The self-organizing map, the Geo-SOM, and relevant variants for geosciences, Comput
650 Geosci, 31, 155–163, https://doi.org/10.1016/j.cageo.2004.06.013, 2005.

Baker, V. R.: Geomorphological understanding of floods, Geomorphology, 10, 139–156, https://doi.org/10.1016/0169-555X(94)90013-2, 1994.

Benito, G. and Hudson, P. F.: Flood hazards: The context of fluvial geomorphology, Geomorphological Hazards and Disaster Prevention, 111–128, https://doi.org/10.1017/CBO9780511807527.010, 2010.

655 Bergen, K. J., Johnson, P. A., De Hoop, M. V., and Beroza, G. C.: Machine learning for data-driven discovery in solid Earth geoscience, Science (1979), 363, https://doi.org/10.1126/SCIENCE.AAU0323/ASSET/E01F2E56-540A-4836-991B-3D3E7652D547/ASSETS/GRAPHIC/363_AAU0323_F5.JPEG, 2019.

Biecek, P., Baniecki, H., and Izdebski, A.: Effects and Importances of Model Ingredients, Journal of Machine Learning Research, 19, 2018.

660 Biecek, P., Gosiewska, A., Baniecki, H., Izdebski, A., and Komosinski, D.: Model Agnostic Instance Level Variable Attributions, R Journal, 10, 395–409, https://doi.org/10.32614/RJ-2018-072, 2019.

Blench 1906-1993, T.: Mobile-bed fluviology : a regime theory treatment of rivers for engineers and hydrologists, Edmonton (Ca.) : University of Alberta press, 1969.

Blöschl, G., Hall, J., Viglione, A., Perdigão, R. A. P., Parajka, J., Merz, B., Lun, D., Arheimer, B., Aronica, G. T., Bilibashi,

665 A., Boháč, M., Bonacci, O., Borga, M., Čanjevac, I., Castellarin, A., Chirico, G. B., Claps, P., Frolova, N., Ganora, D., Gorbachova, L., Gül, A., Hannaford, J., Harrigan, S., Kireeva, M., Kiss, A., Kjeldsen, T. R., Kohnová, S., Koskela, J. J., Ledvinka, O., Macdonald, N., Mavrova-Guirguinova, M., Mediero, L., Merz, R., Molnar, P., Montanari, A., Murphy, C., Osuch, M., Ovcharuk, V., Radevski, I., Salinas, J. L., Sauquet, E., Šraj, M., Szolgay, J., Volpi, E., Wilson, D., Zaimi, K., and Živković, N.: Changing climate both increases and decreases European river floods, Nature 2019 573:7772, 573, 108–111,

670 https://doi.org/10.1038/s41586-019-1495-6, 2019.

Borga, M., Gaume, E., Creutin, J. D., and Marchi, L.: Surveying flash floods: gauging the ungauged extremes, Hydrol Process, 22, 3883–3885, https://doi.org/10.1002/HYP.7111, 2008.

Bormann, H., Pinter, N., and Elfert, S.: Hydrological signatures of flood trends on German rivers: Flood frequencies, flood heights and specific stages, J Hydrol (Amst), 404, 50–66, https://doi.org/10.1016/J.JHYDROL.2011.04.019, 2011.

675 Bracken, L. J. and Croke, J.: The concept of hydrological connectivity and its contribution to understanding runoff-dominated geomorphic systems, Hydrol Process, 21, 1749–1763, https://doi.org/10.1002/hyp.6313, 2007.

Breiman, L.: Random Forests, Mach Learn, 45, 5–32, https://doi.org/10.1023/A:1010933404324, 2001.

Breiman, L.: RANDOM FORESTS, International Journal of Advanced Computer Science and Applications, 7, 1–33, https://doi.org/10.14569/ijacsa.2016.070603, 2016.

680 Brierley, G., Fryirs, K., Reid, H., and Williams, R.: The dark art of interpretation in geomorphology, Geomorphology, 390, 107870, https://doi.org/10.1016/J.GEOMORPH.2021.107870, 2021.

Brierley, G. J. and Fryirs, K. A.: The Use of Evolutionary Trajectories to Guide 'Moving Targets' in the Management of River Futures, River Res Appl, 32, 823–835, https://doi.org/10.1002/rra.2930, 2016.

Buraas, E. M., Renshaw, C. E., Magilligan, F. J., and Dade, W. B.: Impact of reach geometry on stream channel sensitivity to

685 extreme floods, Earth Surf Process Landf, 39, 1778–1789, https://doi.org/10.1002/esp.3562, 2014.

Ceola, S., Laio, F., and Montanari, A.: Global-scale human pressure evolution imprints on sustainability of river systems, Hydrol Earth Syst Sci, 23, 3933–3944, https://doi.org/10.5194/HESS-23-3933-2019, 2019.

Chang, S. E., McDaniels, T. L., Mikawoz, J., and Peterson, K.: Infrastructure failure interdependencies in extreme events: power outage consequences in the 1998 Ice Storm, Natural Hazards, 41, 337–358, https://doi.org/10.1007/s11069-006-9039-

690 4, 2007.

Chen, S. A., Michaelides, K., Grieve, S. W. D., and Singer, M. B.: Aridity is expressed in river topography globally, Nature, 573, 573–577, https://doi.org/10.1038/s41586-019-1558-8, 2019.

Cleveland, W. S.: Robust locally weighted regression and smoothing scatterplots, J Am Stat Assoc, 74, 829–836, https://doi.org/10.1080/01621459.1979.10481038, 1979.

695 Clubb, F. J., Mudd, S. M., Attal, M., Milodowski, D. T., and Grieve, S. W. D.: The relationship between drainage density, erosion rate, and hilltop curvature: Implications for sediment transport processes, J Geophys Res Earth Surf, 121, 1724–1745, https://doi.org/10.1002/2015JF003747, 2016.

Costa, J. A. and Netto, M. L.: Estimating the number of clusters in multivariate data by self-organizing maps, Int J Neural Syst, 9, 195–202, https://doi.org/10.1142/S0129065799000186, 1999.

700 Criss, R. E. and Shock, E. L.: Flood enhancement through flood control, Geology, 29, 875, https://doi.org/10.1130/0091-7613(2001)029<0875:FETFC>2.0.CO;2, 2001.

Croke, J., Fryirs, K., and Thompson, C.: Channel-floodplain connectivity during an extreme flood event: implications for sediment erosion, deposition, and delivery, Earth Surf Process Landf, 38, n/a-n/a, https://doi.org/10.1002/esp.3430, 2013.

Cunderlik, J. M. and Burn, D. H.: Non-stationary pooled flood frequency analysis, J Hydrol (Amst), 276, 210–223,
705 https://doi.org/10.1016/S0022-1694(03)00062-3, 2003.

Death, R. G., Fuller, I. C., and Macklin, M. G.: Resetting the river template: the potential for climate-related extreme floods to transform river geomorphology and ecology, Freshw Biol, 60, 2477–2496, https://doi.org/10.1111/fwb.12639, 2015.

Desta, F., Colbert, J. J., Rentch, J. S., and Gottschalk, K. W.: Aspect induced differences in vegetation, soil, and microclimatic characteristics of an Appalachian watershed | Treesearch, Scientific Journal (JRNL) CASTANEA. 69(2): 92-108., 2004.

710 Dottori, F., Szewczyk, W., Ciscar, J. C., Zhao, F., Alfieri, L., Hirabayashi, Y., Bianchi, A., Mongelli, I., Frieler, K., Betts, R. A., and Feyen, L.: Increased human and economic losses from river flooding with anthropogenic warming, https://doi.org/10.1038/s41558-018-0257-z, 1 September 2018.

Dottori, F., Alfieri, L., Bianchi, A., Skoien, J., and Salamon, P.: A new dataset of river flood hazard maps for Europe and the Mediterranean Basin, Earth Syst Sci Data, 14, 1549–1569, https://doi.org/10.5194/essd-14-1549-2022, 2022.

715 Dresp, B., Wandeto, J. M., and Nyongesa, H. O.: Données image et décision: détection automatique de variations dans des séries temporelles par réseau de Kohonen-- Using the quantization error from Self-Organizing Map (SOM) output for fast detection of critical variations in image time series, Des données à la décision-From data to decisions , 2, 2018.

FEMA: Reducing Flood Effects in Critical Facilities, HSFE60-13-, 1–11, 2013.

Physiographic divisions of the conterminous U. S.: https://water.usgs.gov/lookup/getspatial?physio, last access: 18 May 2023.

720 Fisher, A., Rudin, C., and Dominici, F.: All Models are Wrong, but Many are Useful: Learning a Variable's Importance by Studying an Entire Class of Prediction Models Simultaneously, Journal of Machine Learning Research, 20, 2018.

Fytilis, N. and Rizzo, D. M.: Coupling self-organizing maps with a Naïve Bayesian classifier: Stream classification studies using multiple assessment data, Water Resour Res, 49, 7747–7762, https://doi.org/10.1002/2012WR013422, 2013.

Geem, Z. W., Tseng, C. L., Kim, J., and Bae, C.: Trenchless Water Pipe Condition Assessment Using Artificial Neural

725 Network, Pipelines 2007: Advances and Experiences with Trenchless Pipeline Projects - Proceedings of the ASCE International Conference on Pipeline Engineering and Construction, 1–9, https://doi.org/10.1061/40934(252)26, 2007.

Granato ggranato, G. E.: Prepared in cooperation with the Department of Transportation Federal Highway Administration Office of Project Development and Environmental Review Estimating Basin Lagtime and Hydrograph-Timing Indexes Used to Characterize Stormflows for Runoff-Quality Analysis Scientific Investigations Report 2012-5110, n.d.

730 Grill, G., Lehner, B., Thieme, M., Geenen, B., Tickner, D., Antonelli, F., Babu, S., Borrelli, P., Cheng, L., Crochetiere, H., Ehalt Macedo, H., Filgueiras, R., Goichot, M., Higgins, J., Hogan, Z., Lip, B., McClain, M. E., Meng, J., Mulligan, M., Nilsson, C., Olden, J. D., Opperman, J. J., Petry, P., Reidy Liermann, C., Sáenz, L., Salinas-Rodríguez, S., Schelle, P., Schmitt, R. J. P., Snider, J., Tan, F., Tockner, K., Valdujo, P. H., van Soesbergen, A., and Zarfl, C.: Mapping the world's free-flowing rivers, Nature, 569, 215–221, https://doi.org/10.1038/s41586-019-1111-9, 2019.

735 Gupta, V. K. and Dawdy, D. R.: Physical interpretations of regional variations in the scaling exponents of flood quantiles, Hydrol Process, 9, 347–361, https://doi.org/10.1002/hyp.3360090309, 1995.

Hassan, M. A., Egozi, R., and Parker, G.: Experiments on the effect of hydrograph characteristics on vertical grain sorting in gravel bed rivers, Water Resour Res, 42, 9408, https://doi.org/10.1029/2005WR004707, 2006.

Hattermann, F. F., Huang, S., Burghoff, O., Willems, W., Österle, H., Büchner, M., and Kundzewicz, Z.: Modelling flood

740 damages under climate change conditions-a case study for Germany, Natural Hazards and Earth System Sciences, 14, 3151–3169, https://doi.org/10.5194/nhess-14-3151-2014, 2014.

Houser, C., Lehner, J., and Smith, A.: The Field Geomorphologist in a Time of Artificial Intelligence and Machine Learning, https://doi.org/10.1080/24694452.2021.1985956, 112, 1260–1277, https://doi.org/10.1080/24694452.2021.1985956, 2022.

Hurvich, C. M., Simonoff, J. S., and Tsai, C.-L.: Smoothing parameter selection in nonparametric regression using an improved

745 Akaike information criterion, J R Stat Soc Series B Stat Methodol, 60, 271–293, https://doi.org/10.1111/1467-9868.00125, 1998.

GAGES-II: Geospatial Attributes of Gages for Evaluating Streamflow: https://water.usgs.gov/GIS/metadata/usgswrd/XML/gagesII_Sept2011.xml, last access: 7 February 2022.

Kalantari, Z., Ferreira, C. S. S., Koutsouris, A. J., Ahmer, A. K., Cerdà, A., and Destouni, G.: Assessing flood probability for

750 transportation infrastructure based on catchment characteristics, sediment connectivity and remotely sensed soil moisture, Science of the Total Environment, 661, 393–406, https://doi.org/10.1016/j.scitotenv.2019.01.009, 2019.

Karagiannis, G. M., Chondrogiannis, S., Krausmann, E., and Turksezer, Z. I.: Power grid recovery after natural hazard impact, https://doi.org/10.2760/87402, 2017.

Karpatne, A., Ebert-Uphoff, I., Ravela, S., Babaie, H. A., and Kumar, V.: Machine Learning for the Geosciences: Challenges

755 and Opportunities, IEEE Trans Knowl Data Eng, 31, 1544–1554, https://doi.org/10.1109/TKDE.2018.2861006, 2019.

Khanam, M., Sofia, G., Koukoula, M., Lazin, R., Nikolopoulos, E. I., Shen, X., and Anagnostou, E. N.: Impact of compound flood event on coastal critical infrastructures considering current and future climate, Natural Hazards and Earth System Sciences, 21, https://doi.org/10.5194/nhess-21-587-2021, 2021.

Kohonen, T.: Self-organized formation of topologically correct feature maps, Biological Cybernetics 1982 43:1, 43, 59–69,
760 https://doi.org/10.1007/BF00337288, 1982.

Kohonen, T.: Self-Organizing Maps, Springer Series in Information Sciences, Vol. 30, Third Extended Edition, 501 pp, n.d.

Lane, S. N., Tayefi, V., Reid, S. C., Yu, D., and Hardy, R. J.: Interactions between sediment delivery, channel change, climate change and flood risk in a temperate upland environment, Earth Surf Process Landf, 32, 429–446, https://doi.org/10.1002/esp.1404, 2007.

765 Li, Y., Wright, D. B., and Byrne, P. K.: The Influence of Tropical Cyclones on the Evolution of River Conveyance Capacity in Puerto Rico, Water Resour Res, 56, https://doi.org/10.1029/2020WR027971, 2020.

Lisenby, P. E. and Fryirs, K. A.: Catchment- and reach-scale controls on the distribution and expectation of geomorphic channel adjustment, Water Resour Res, 52, 3408–3427, https://doi.org/10.1002/2015WR017747, 2016.

Lisenby, P. E., Croke, J., and Fryirs, K. A.: Geomorphic effectiveness: a linear concept in a non-linear world, Earth Surf
770 Process Landf, 43, 4–20, https://doi.org/10.1002/esp.4096, 2018.

Luo, W., Jasiewicz, J., Stepinski, T., Wang, J., Xu, C., and Cang, X.: Spatial association between dissection density and environmental factors over the entire conterminous United States, Geophys Res Lett, 43, 692–700, https://doi.org/10.1002/2015GL066941, 2016.

Mallakpour, I. and Villarini, G.: The changing nature of flooding across the central United States, Nat Clim Chang, 5, 250–
775 254, https://doi.org/10.1038/nclimate2516, 2015.

McEvoy, D., Ahmed, I., and Mullett, J.: The impact of the 2009 heat wave on Melbourne's critical infrastructure, Local Environ, 17, 783–796, https://doi.org/10.1080/13549839.2012.678320, 2012.

Merz, B., Vorogushyn, S., Uhlemann, S., Delgado, J., and Hundecha, Y.: HESS Opinions &quot;More efforts and scientific rigour are needed to attribute trends in flood time series&quot;, Hydrol Earth Syst Sci, 16, 1379–1387,
780 https://doi.org/10.5194/hess-16-1379-2012, 2012.

Milly, P. C. D., Wetherald, R. T., Dunne, K. A., and Delworth, T. L.: Increasing risk of great floods in a changing climate, Nature, 415, 514–517, https://doi.org/10.1038/415514a, 2002.

Molnar, C.: Interpretable Machine Learning: A Guide for Making Black Box Models Explainable, 2nd ed., 2022.

Molnar, C. and Schratz, P.: Interpretable Machine Learning, Annals of Applied Statistics, 2, 916–954,
785 https://doi.org/10.1214/07-AOAS148, 2008.

Mostofi Zadeh, S., Burn, D. H., and O'Brien, N.: Detection of trends in flood magnitude and frequency in Canada, J Hydrol Reg Stud, 28, 100673, https://doi.org/10.1016/j.ejrh.2020.100673, 2020.

Munoz, S. E., Giosan, L., Therrell, M. D., Remo, J. W. F., Shen, Z., Sullivan, R. M., Wiman, C., O'Donnell, M., and Donnelly, J. P.: Climatic control of Mississippi River flood hazard amplified by river engineering, Nature, 556, 95–98,
790 https://doi.org/10.1038/nature26145, 2018.

Naylor, L. A., Spencer, T., Lane, S. N., Darby, S. E., Magilligan, F. J., Macklin, M. G., and Möller, I.: State of Science Stormy geomorphology: geomorphic contributions in an age of climate extremes, https://doi.org/10.1002/esp.4062, 2016.

Neuhold, C., Stanzel, P., and Nachtnebel, H. P.: Incorporating river morphological changes to flood risk assessment: Uncertainties, methodology and application, Natural Hazards and Earth System Science, 9, 789–799,
795 https://doi.org/10.5194/nhess-9-789-2009, 2009.

Pacheco, F. S., Miranda, M., Pezzi, L. P., Assireu, A., Marinho, M. M., Malafaia, M., Reis, A., Sales, M., Correia, G., Domingos, P., Iwama, A., Rudorff, C., Oliva, P., and Ometto, J. P.: Water quality longitudinal profile of the Paraíba do Sul River, Brazil during an extreme drought event, Limnol Oceanogr, 62, S131–S146, https://doi.org/10.1002/LNO.10586, 2017.

Pfeiffer, A. M., Collins, B. D., Anderson, S. W., Montgomery, D. R., and Istanbulluoglu, E.: River Bed Elevation Variability
800 Reflects Sediment Supply, Rather Than Peak Flows, in the Uplands of Washington State, Water Resour Res, 55, 6795–6810, https://doi.org/10.1029/2019WR025394, 2019.

Pinter, N., Thomas, R., and Wlosinski, J. H.: Assessing flood hazard on dynamic rivers, Eos, Transactions American Geophysical Union, 82, 333–333, https://doi.org/10.1029/01EO00199, 2001.

Pinter, N., Van der Ploeg, R. R., Schweigert, P., and Hoefer, G.: Flood magnification on the River Rhine, Hydrol Process, 20,
805 147–164, https://doi.org/10.1002/hyp.5908, 2006a.

Pinter, N., Ickes, B. S., Wlosinski, J. H., and van der Ploeg, R. R.: Trends in flood stages: Contrasting results from the Mississippi and Rhine River systems, J Hydrol (Amst), 331, 554–566, https://doi.org/10.1016/J.JHYDROL.2006.06.013, 2006b.

Pinter, N., Jemberie, A. A., Remo, J. W. F., Heine, R. A., and Ickes, B. S.: Flood trends and river engineering on the Mississippi
810 River system, Geophys. Res. Lett, 35, 23404, https://doi.org/10.1029/2008GL035987, 2008.

Rahmati, O., Darabi, H., Haghighi, A. T., Stefanidis, S., Kornejady, A., Nalivan, O. A., and Bui, D. T.: Urban flood hazard modeling using self-organizing map neural network, Water (Switzerland), 11, https://doi.org/10.3390/w11112370, 2019.

Rathburn, S. L., Bennett, G. L., Wohl, E. E., Briles, C., McElroy, B., and Sutfin, N.: The fate of sediment, wood, and organic carbon eroded during an extreme flood, Colorado Front Range, USA, Geology, 45, 499–502,
815 https://doi.org/10.1130/G38935.1, 2017.

Reis, A. H.: Constructal view of scaling laws of river basins, Geomorphology, 78, 201–206, https://doi.org/10.1016/j.geomorph.2006.01.015, 2006.

Riese, F. M. and Keller, S.: Introducing a framework of self-organizing maps for regression of soil moisture with hyperspectral data, International Geoscience and Remote Sensing Symposium (IGARSS), 2018-July, 6151–6154,
820 https://doi.org/10.1109/IGARSS.2018.8517812, 2018.

Riese, F. M. and Keller, S.: SuSi: Supervised Self-Organizing Maps for Regression and Classification in Python, Remote Sensing 2020, Vol. 12, Page 7, 12, 7, 2019.

Rinaldi, M., Amponsah, W., Benvenuti, M., Borga, M., Comiti, F., Lucía, A., Marchi, L., Nardi, L., Righini, M., and Surian, N.: An integrated approach for investigating geomorphic response to extreme events: methodological framework and
825 application to the October 2011 flood in the Magra River catchment, Italy, Earth Surf Process Landf, 41, 835–846, https://doi.org/10.1002/esp.3902, 2016.

Ruiz-Villanueva, V., Badoux, A., Rickenmann, D., Böckli, M., Schläfli, S., Steeb, N., Stoffel, M., and Rickli, C.: Impacts of a large flood along a mountain river basin: The importance of channel widening and estimating the large wood budget in the upper Emme River (Switzerland), Earth Surface Dynamics, 6, 1115–1137, https://doi.org/10.5194/esurf-6-1115-2018, 2018.

830 Saco, P. M. and Kumar, P.: Kinematic dispersion in stream networks 1. Coupling hydraulic and network geometry, Water Resour Res, 38, 26–1, https://doi.org/10.1029/2001WR000695, 2002.

Saghafian, B.: Time of Concentration and Travel Time in Watersheds, Water Encyclopedia, 469–472, https://doi.org/10.1002/047147844X.SW1033, 2005.

Saharia, M., Kirstetter, P. E., Vergara, H., Gourley, J. J., Hong, Y., and Giroud, M.: Mapping Flash Flood Severity in the
835 United States, J Hydrometeorol, 18, 397–411, https://doi.org/10.1175/JHM-D-16-0082.1, 2017.

Sarker, I. H.: Deep Learning: A Comprehensive Overview on Techniques, Taxonomy, Applications and Research Directions, SN Comput Sci, 2, 1–20, https://doi.org/10.1007/S42979-021-00815-1/FIGURES/6, 2021.

Schlef, K. E., Moradkhani, H., and Lall, U.: Atmospheric Circulation Patterns Associated with Extreme United States Floods Identified via Machine Learning, Sci Rep, 9, 7171, https://doi.org/10.1038/s41598-019-43496-w, 2019.

840 Scorpio, V., Crema, S., Marra, F., Righini, M., Ciccarese, G., Borga, M., Cavalli, M., Corsini, A., Marchi, L., Surian, N., and Comiti, F.: Basin-scale analysis of the geomorphic effectiveness of flash floods: A study in the northern Apennines (Italy), Science of The Total Environment, 640–641, 337–351, https://doi.org/10.1016/j.scitotenv.2018.05.252, 2018.

Seo, Y. and Schmidt, A. R.: The effect of rainstorm movement on urban drainage network runoff hydrographs, Hydrol Process, 26, 3830–3841, https://doi.org/10.1002/HYP.8412, 2012.

845 Seo, Y., Hwang, J., and Noh, S. J.: Analysis of Urban Drainage Networks Using Gibbs' Model: A Case Study in Seoul, South Korea, Water 2015, Vol. 7, Pages 4129-4143, 7, 4129–4143, https://doi.org/10.3390/W7084129, 2015.

Shen, X., Mei, Y., and Anagnostou, E. N.: A comprehensive database of flood events in the contiguous United States from 2002 to 2013, Bull Am Meteorol Soc, 98, 1493–1502, https://doi.org/10.1175/BAMS-D-16-0125.1, 2017.

Slater, L. J.: To what extent have changes in channel capacity contributed to flood hazard trends in England and Wales?, Earth
850 Surf Process Landf, 41, 1115–1128, https://doi.org/10.1002/esp.3927, 2016.

Slater, L. J. and Villarini, G.: Recent trends in U.S. flood risk, Geophys Res Lett, 43, 12,428-12,436, https://doi.org/10.1002/2016GL071199, 2016.

Slater, L. J., Singer, M. B., and Kirchner, J. W.: Hydrologic versus geomorphic drivers of trends in flood hazard, Geophys Res Lett, 42, 370–376, https://doi.org/10.1002/2014GL062482, 2015.

855   Slater, L. J., Khouakhi, A., and Wilby, R. L.: River channel conveyance capacity adjusts to modes of climate variability, Sci
        Rep, 9, 1–10, https://doi.org/10.1038/s41598-019-48782-1, 2019.

        Slater, L. J., Singer, M. B., and Kirchner, J. W.: Supporting Information for Hydrologic versus geomorphic drivers of trends
        in flood hazard, Geophysical Research Letters, n.d.

        Smith, J. A., Baeck, M. L., Morrison, J. E., Sturdevant-Rees, P., Turner-Gillespie, D. F., and Bates, P. D.: The regional
860   hydrology of extreme floods in an urbanizing drainage basin, J Hydrometeorol, 3, 267–282, https://doi.org/10.1175/1525-
        7541(2002)003<0267:TRHOEF>2.0.CO;2, 2002.

        Smith, J. A., Baeck, M. L., Meierdiercks, K. L., Nelson, P. A., Miller, A. J., and Holland, E. J.: Field studies of the storm event
        hydrologic response in an urbanizing watershed, Water Resour Res, 41, https://doi.org/10.1029/2004WR003712, 2005.

        Smith, M. B., Koren, V. I., Zhang, Z., Reed, S. M., Pan, J. J., and Moreda, F.: Runoff response to spatial variability in
865   precipitation: An analysis of observed data, J Hydrol (Amst), 298, 267–286, https://doi.org/10.1016/j.jhydrol.2004.03.039,
        2004.

        Sofia, G.: Combining geomorphometry, feature extraction techniques and Earth-surface processes research: The way forward,
        Geomorphology, 355, 107055, https://doi.org/10.1016/J.GEOMORPH.2020.107055, 2020.

        Sofia, G. and Nikolopoulos, E. I.: Floods and rivers: a circular causality perspective, Sci Rep, 10,
870   https://doi.org/10.1038/s41598-020-61533-x, 2020a.

        Sofia, G. and Nikolopoulos, E. I.: Floods and rivers: a circular causality perspective, Sci Rep, 10,
        https://doi.org/10.1038/s41598-020-61533-x, 2020b.

        Sofia, G., Nikolopoulos, E., and Slater, L.: It's Time to Revise Estimates of River Flood Hazards, Eos (Washington DC), 101,
        https://doi.org/10.1029/2020EO141499, 2020.

875   Stark, C. P., Barbour, J. R., Hayakawa, Y. S., Hattanji, T., Hovius, N., Chen, H., Lin, C. W., Horng, M. J., Xu, K. Q., and
        Fukahata, Y.: The climatic signature of incised river meanders, Science (1979), 327, 1497–1501,
        https://doi.org/10.1126/science.1184406, 2010.

        Stefanovič, P. and Kurasova, O.: Visual analysis of self-organizing maps, Nonlinear Analysis: Modelling and Control, 16,
        488–504, https://doi.org/10.15388/na.16.4.14091, 2011.

880   Stott, T.: Review of research in fluvial geomorphology 2010–2011:, http://dx.doi.org/10.1177/0309133313477124, 37, 248–
        258, https://doi.org/10.1177/0309133313477124, 2013.

        Stover, S. C. and Montgomery, D. R.: Channel change and flooding, Skokomish River, Washington, J Hydrol (Amst), 243,
        272–286, https://doi.org/10.1016/S0022-1694(00)00421-2, 2001.

        Surian, N., Righini, M., Lucía, A., Nardi, L., Amponsah, W., Benvenuti, M., Borga, M., Cavalli, M., Comiti, F., Marchi, L.,
885   Rinaldi, M., and Viero, A.: Channel response to extreme floods: Insights on controlling factors from six mountain rivers in
        northern Apennines, Italy, Geomorphology, 272, 78–91, https://doi.org/10.1016/j.geomorph.2016.02.002, 2016.

        Swenson, L. M. and Grotjahn, R.: Using Self-Organizing Maps to Identify Coherent CONUS Precipitation Regions, J Clim,
        32, 7747–7761, https://doi.org/10.1175/JCLI-D-19-0352.1, 2019.
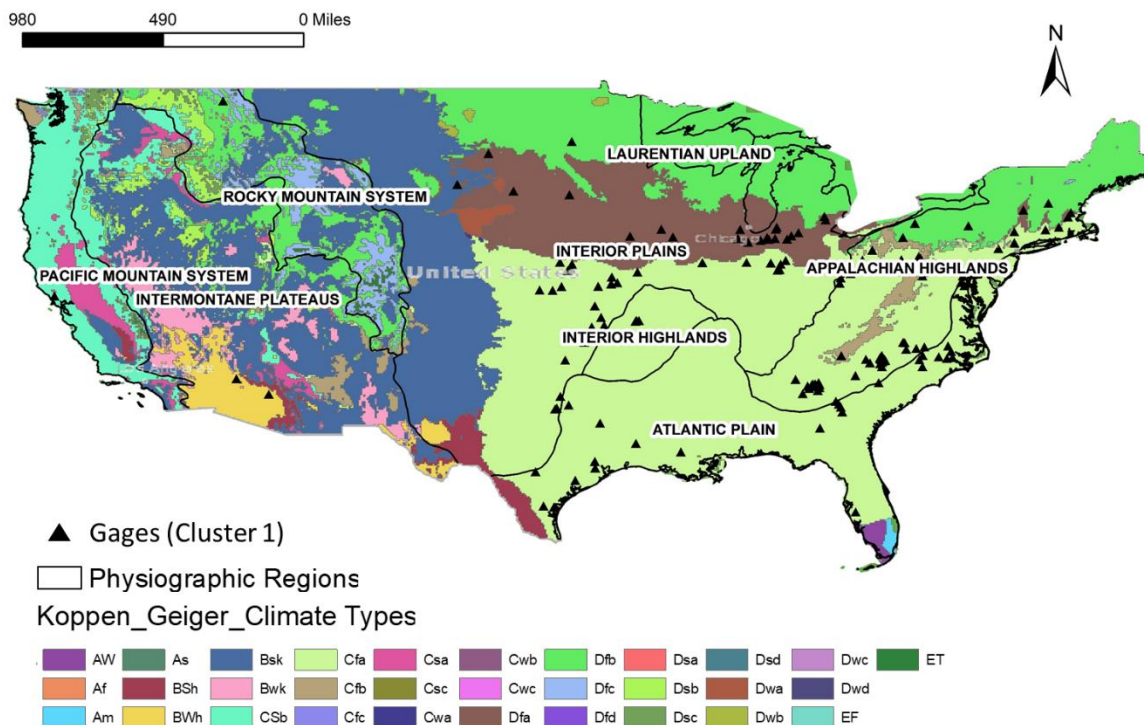
Székely, G. J., Rizzo, M. L., and Bakirov, N. K.: MEASURING AND TESTING DEPENDENCE BY CORRELATION OF

890   DISTANCES, The Annals of Statistics, 35, 2769–2794, https://doi.org/10.1214/009053607000000505, 2007.

Tate, E.: Déjà Vu All Over Again: Trends in Flood Drivers Point to Continuing Vulnerability, Environment: Science and
Policy for Sustainable Development, 61, 50–55, https://doi.org/10.1080/00139157.2019.1637688, 2019.

Torres-Matallana, J. A.: Spatial Watershed Aggregation and Spatial Drainage Network Analysis, 2016.

Ultsch, A. and Lötsch, J.: Machine-learned cluster identification in high-dimensional data, J Biomed Inform, 66, 95–104,

895   https://doi.org/10.1016/j.jbi.2016.12.011, 2017.

Valentine, A. and Kalnins, L.: An introduction to learning algorithms and potential applications in geomorphometry and Earth
surface dynamics, Earth Surface Dynamics, 4, 445–460, https://doi.org/10.5194/esurf-4-445-2016, 2016.

Vesanto, J. and Alhoniemi, E.: Clustering of the self-organizing map, IEEE Trans Neural Netw, 11, 586–600,
https://doi.org/10.1109/72.846731, 2000.

900   Villarini, G. and Smith, J. A.: Flood peak distributions for the eastern United States, Water Resour Res, 46, 6504,
https://doi.org/10.1029/2009WR008395, 2010.

Vincent, L., Vincent, L., and Soille, P.: Watersheds in Digital Spaces: An Efficient Algorithm Based on Immersion
Simulations, IEEE Trans Pattern Anal Mach Intell, 13, 583–598, https://doi.org/10.1109/34.87344, 1991.

Wandeto, J. M. and Dresp-Langley, B.: Reprint of: The quantization error in a Self-Organizing Map as a contrast and colour

905   specific   indicator   of   single-pixel   change   in   large   random   patterns,   Neural   Networks,   120,   116–128,
https://doi.org/10.1016/j.neunet.2019.09.017, 2019.

Wang, H., Chen, X., Moss, R. H., Stanley, R. J., Stoecker, W. V., Celebi, M. E., Szalapski, T. M., Malters, J. M., Grichnik, J.
M., Marghoob, A. A., Rabinovitz, H. S., and Menzies, S. W.: Watershed segmentation of dermoscopy images using a
watershed technique, Skin Res Technol, 16, 378, https://doi.org/10.1111/J.1600-0846.2010.00445.X, 2010.

910   Wehrens, M. R.: Package ' kohonen ,' 2019.

Wehrens, R. and Buydens, L. M. C.: Self- and Super-organizing Maps in R: The kohonen Package, Journal of Statistical
Software; Vol 1, Issue 5 (2007) , 2007.

Wehrens, R. and Kruisselbrink, J.: Flexible Self-Organizing Maps in kohonen 3.0, Journal of Statistical Software; Vol 1, Issue
7 (2018) , 2018.

915   Wei, P., Lu, Z., and Song, J.: Variable importance analysis: A comprehensive review, Reliab Eng Syst Saf, 142, 399–432,
https://doi.org/10.1016/j.ress.2015.05.018, 2015.

Wicherski, W., Dethier, D. P., and Ouimet, W. B.: Erosion and channel changes due to extreme flooding in the Fourmile Creek
catchment, Colorado, Geomorphology, 294, 87–98, https://doi.org/10.1016/j.geomorph.2017.03.030, 2017.

Wohl, E.: Forgotten Legacies: Understanding and Mitigating Historical Human Alterations of River Corridors, Water Resour

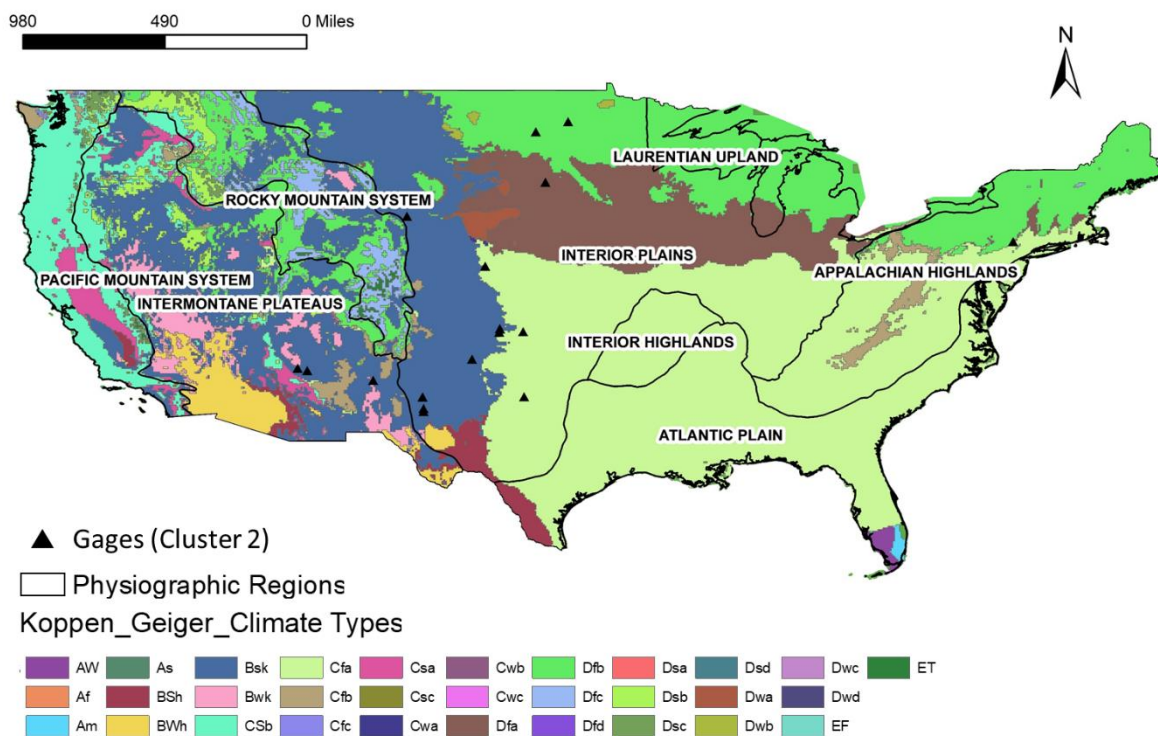920   Res, 55, 5181–5201, https://doi.org/10.1029/2018WR024433, 2019.

Wohl, E., Brierley, G., Cadol, D., Coulthard, T. J., Covino, T., Fryirs, K. A., Grant, G., Hilton, R. G., Lane, S. N., Magilligan, F. J., Meitzen, K. M., Passalacqua, P., Poeppl, R. E., Rathburn, S. L., and Sklar, L. S.: Connectivity as an emergent property of geomorphic systems, Earth Surf Process Landf, 44, 4–26, https://doi.org/10.1002/esp.4434, 2019.

Woods, R.: Rain • Distributed • Hillslope • Channel _• Q (t), 35, 2469–2485, 1999.

925 Woods, R. and Sivapalan, M.: A synthesis of space-time variability in storm response: Rainfall, runoff generation, and routing, Water Resour Res, 35, 2469–2485, https://doi.org/10.1029/1999WR900014, 1999.

Wu, Y. and Li, Q.: The Algorithm of Watershed Color Image Segmentation Based on Morphological Gradient, Sensors (Basel), 22, https://doi.org/10.3390/S22218202, 2022.

Zanchetta, A. D. L. and Coulibaly, P.: Hybrid Surrogate Model for Timely Prediction of Flash Flood Inundation Maps Caused
930 by Rapid River Overflow, Forecasting 2022, Vol. 4, Pages 126-148, 4, 126–148, https://doi.org/10.3390/FORECAST4010007, 2022.

Zhang, S., Guo, Y., and Wang, Z.: Correlation between flood frequency and geomorphologic complexity of rivers network – A case study of Hangzhou China, J Hydrol (Amst), 527, 113–118, https://doi.org/10.1016/J.JHYDROL.2015.04.060, 2015.

Zhang, Y., Smith, J. A., and Baeck, M. L.: The hydrology and hydrometeorology of extreme floods in the Great Plains of
935 Eastern Nebraska, Adv Water Resour, 24, 1037–1049, https://doi.org/10.1016/S0309-1708(01)00037-9, 2001.

Ziervogel, G., New, M., Archer van Garderen, E., Midgley, G., Taylor, A., Hamann, R., Stuart-Hill, S., Myers, J., and Warburton, M.: Climate change impacts and adaptation in South Africa, Wiley Interdiscip Rev Clim Change, 5, 605–620, https://doi.org/10.1002/wcc.295, 2014.

Zischg, A. P., Hofer, P., Mosimann, M., Röthlisberger, V., Ramirez, J. A., Keiler, M., and Weingartner, R.: Flood risk
940 (d)evolution: Disentangling key drivers of flood risk change with a retro-model experiment, Science of the Total Environment, 639, 195–207, https://doi.org/10.1016/j.scitotenv.2018.05.056, 2018.

Appendix A

945

e

950

955

Figure A1: Gages with clustering identification assigned by SOM unsupervised clustering (a-l)